**Performance characteristics and
design of voltage references**

by

Yunting Yin

A thesis submitted to the graduate faculty

in partial fulfillment of the requirements for the degree of

MASTER OF SCIENCE

Major: Electrical Engineering

Program of Study Committee:
Randall L. Geiger, Major Professor
Degang J. Chen
Yong Guan

Iowa State University

Ames, Iowa

2017

DEDICATION

To my family

TABLE OF CONTENTS

LIST OF FIGURES

LIST OF TABLES

ACKNOWLEDGEMENTS

ABSTRACT

Integrated circuits comprise the core of essentially all electronic systems. In the design of many integrated circuits, one task of the design engineer is to provide accurate voltages to sub blocks in the circuit structure. The circuits that provide these voltages are often referred to as voltage references. A widely used class of voltage references that typically have low supply, process, and temperature sensitivities are bandgap references whose output voltage is dominated by the bandgap voltage of silicon. Though several structurally different bandgap reference circuits are widely used in industry, there is little in the literature that focuses on how the performance of these circuits can be optimized or how the performance of different bandgap circuits compare. The task of optimization and comparison is complicated by the realization that each of the bandgap circuits themselves have several degrees of freedom in the design. In this work, a metric for fairly comparing the basic performance of different bandgap references based upon the normalized second-order temperature derivative is introduced. This metric is used to compare the performance of several of the most popular bandgap reference circuits that are used in the production. The comparisons show that even though the structure of these reference circuits are fundamentally different and even though each circuit has several degrees of design freedom, the normalized temperature coefficients of all circuits in the comparison group at a fixed operating temperature are the same. The comparisons also show that the designer

cannot optimize the basic performance of any of these circuits through judicious utilization of the degrees of design freedom.

In this work, a new very low power voltage reference obtained by replacing the diode-connected bipolar transistors in a basic bandgap circuit with diode-connected MOS transistors operating in deep weak inversion is also discussed. An analytical formulation of the weak-inversion MOS voltage reference shows that the MOSFET-based structure has even lower temperature sensitivity than the basic bandgap circuits. The issue of practicality of the MOS-based reference is, however, of concern since the extremely low currents appear to create the need for very large resistors which are not realistically available in most standard CMOS processes.

Key word: second order coefficient, bandgap reference circuit, PN junction, MOSFET

CHAPTER I INTRODUCTION

In modern industry chip design, accurate, low-power, supply-independent, and temperature stable voltage references are essential for many designs. Since the chip may go through a variety of temperature ranges during normal operation, temperature stability is often particularly important. Maintaining temperature independence is inherently a challenging problem since the electrical properties of transistors and resistors are heavily influenced by temperature.

1.1 Voltage Reference

In Wikipedia, a voltage reference is defined as "A voltage reference is an electronic device that ideally produces a fixed (constant) voltage irrespective of the loading on the device, power supply variations, temperature changes, and the passage of time" [1]. Although an ideal voltage reference would provide a fixed value of output voltage independent of temperature, supply voltage, process parameters, and other environmental variables, even the best voltage references available depend a little on these factors.

The earliest voltage references were evolved from the field of metrology and were comprised of a wet-chemical cell often referred to as a Clark Cell. These cells have zinc or zinc amalgam anodes and mercury cathodes and are immersed in a saturated aqueous solution of zinc sulfate, with a paste comprised of mercurous sulfate as a depolarizer [2]. These voltage references had a specific temperature requirement and also exhibited a temperature slope. In about 1905, applications using the Clark cell were often replaced by the Weston cell [3]. The latter is more temperature-

independent. Other types of voltage references have been used in metrology and are based upon Zener diodes, Josephson junctions and mercury batteries. At first, people just wanted to obtain some standard voltage criteria and calibration was used to enhance performance much like was common practice for other kinds of metrology such as that used to establish length and weight standards. Many of the earlier voltage references were based upon chemistry of the materials used to make the reference and the resulting references were not practical for extensive utilization in cost-sensitive electronic systems.

In contrast, solid-state references are based on physical properties of devices. They are often smaller, less expensive, and can be embedded in a cost-effective way in many electronic circuits and systems. The most of common solid-state references are based upon either the electrical properties of a Zener diode or the bandgap characteristics of silicon expressed through the electrical properties of PN junctions. The PN junctions are invariably associated with junction diodes or bipolar transistors. Voltage references based upon the bandgap voltage of silicon are descriptively termed bandgap references.

The Zener diode has some diode properties but references based upon Zener diodes are based upon the nondestructive breakdown voltage that can be used to obtain a reasonably constant output voltage. Since the Zener diode operating in breakdown can tolerate a large range of reverse currents and still keep the voltage drop quite constant, they can be used to build simple low-cost voltage references. Zener diodes

can be designed to operate at different breakdown voltages. Unfortunately, good Zener diodes are often not available in many of the widely-used CMOS processes.

Bandgap references are widely used in industry and can be built in most standard semiconductor processes. Most bandgap references evolved by creating the weighted sum of two internally generated voltages, one with a positive temperature coefficient and the other with a negative temperature coefficient. By adjusting the weight properly, the derivative can be forced to vanish at a predetermined temperature. Several of the more popular bandgap circuits exhibit an output voltage around 1.25 V (close to the theoretical 1.22 eV bandgap of silicon at 0 K). This circuit concept was first published by David Hilbiber in 1964 [1]. Bob Widlar, Paul Brokaw and others followed up with other commercially successful versions [1].

The most basic structure of a voltage reference is shown in Figure 1.
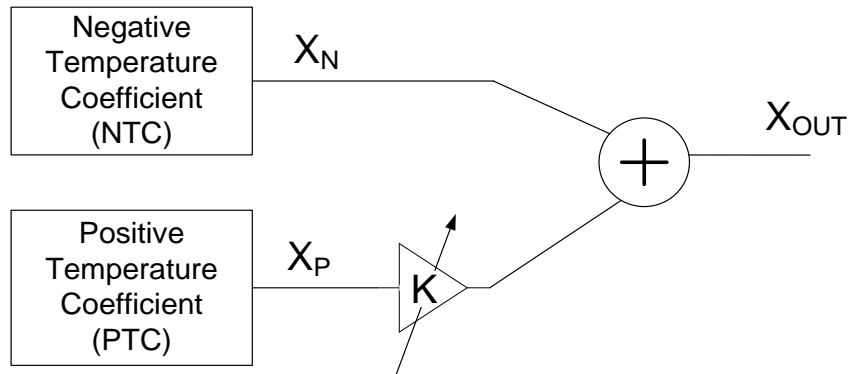
Figure 1 Standard idea of voltage reference

In this structure, two voltages, X_N and X_P, which have opposite polarity temperature coefficients are generated. The temperature coefficient of X_N is negative and satisfies the relationship $\frac{\partial X_N(T)}{\partial T} = \Psi_N < 0$ The temperature coefficient of X_P satisfies the relationship $\frac{\partial X_P(T)}{\partial T} = \Psi_P > 0$. It follows that the output can be expressed as:

$$X_{OUT} = X_N + KX_P \tag{1}$$

It directly follows from equation (1) that:

$$\frac{\partial X_{OUT}}{\partial T} = \frac{\partial X_N}{\partial T} + K\frac{\partial X_P}{\partial T} \tag{2}$$

The gain K is selected so that the derivative vanishes at a predetermined temperature that is descriptively termed the inflection temperature, T_{INF}. It thus follows that K must satisfy the equation (3):

$$\frac{\partial X_{OUT}}{\partial T}\bigg|_{T=T_{INF}} = \frac{\partial X_N}{\partial T}\bigg|_{T=T_{INF}} + K\frac{\partial X_P}{\partial T}\bigg|_{T=T_{INF}} = 0 \tag{3}$$

From the equation (3), the value of K can be expressed like this:

$$K = -\frac{\frac{\partial X_N}{\partial T}\big|_{T=T_{INF}}}{\frac{\partial X_N}{\partial T}\big|_{T=T_{INF}}} \tag{4}$$

The value of K is often dependent upon several process parameters that may change from the nominal value during fabrication of the circuit. This will cause a shift in T_{INF} from the desired value. If this shift is unacceptable, the circuit can be trimmed after manufacturing.

1.2 Introduction of Bandgap Reference Circuit

Bandgap references have been widely used since the mid 1970's. The seminal creation on references is attributable to Widlar [4] who published some of the first papers on the subject in 1969 and 1971 while working at National Semiconductor. His work in 1971 is a basic bandgap structure. Another early paper on the topic is that of Brokow [6] in 1974 who was working at Analog Devices at the time although the basic ideas of the Brokow work appears to have been published earlier by Widlar. In its most basic form, a bandgap reference has a voltage-temperature relationship that has a single inflection point although some of the better voltage references may have two or more

inflection points or may use some other forms of curvature compensation to reduce the dependence of temperature on the output. The basic bandgap references derive their name from the observation that the output voltage of such references is dominantly dependent upon and often approximately proportional to the bandgap voltage of silicon, V_{G0}. Though the concept of a bandgap circuit is often attributed to Widlar [5], the term "bandgap circuit" was coined after the seminal work of Widlar was reported.

Three of the major concerns in the design of voltage references are the effects of the power supply, the effects of temperature, and the sensitivity of the output voltage to model and design parameters. One of the simplest references is two resistors connected in series and biased with a dc voltage source, VDD. With this structure, a 10% change in VDD would cause a 10% change in the reference output. This high supply voltage sensitivity is unacceptable in most applications. A reference that is somewhat less sensitive to the supply voltage is a single resistor connected in series with a diode or a diode connected resistor such as shown in Figure 2.
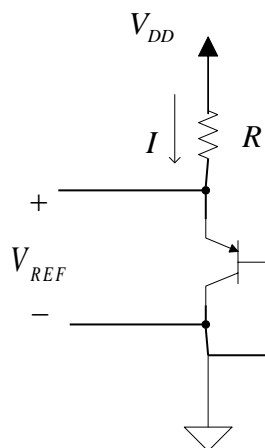
Figure 2 PN junction voltage reference

Similar to the analysis in [7] it can be readily shown that if the saturation current density of the diode is $I_S = 3.26 \times 10^{-16} A$, the supply voltage is 5V, and the resistor is

2000 Ω, then a increase of 10% change in V_{DD} at the fixed temperature creates only a

0.387% change in the V_{REF}. Though the supply sensitivity is considerably reduced

with this simple circuit, it is still too large for many applications. Replacing the diode

with a diode-connected MOSFET would also give better V_{DD} sensitivity than the simple

resistive divider structure, but it would typically not be as good as with the diode. A

cascoded MOSFET would offer some improvements in supply sensitivity but even that

would not be adequate in most applications. In this paper, the major focus will be on

the effects of temperature on the performance of the reference though the circuits that

will be discussed also have low supply voltage sensitivity.

Some of the earlier work on voltage references focused on compensating the

negative temperature coefficient of a PN junction operating with nearly constant current

with the positive temperature coefficient available in some resistors. This approach is

consistent with the concepts shown in Figure 3. As an example, with a temperature

coefficient of a PN junction of -2mV/℃ and a temperature coefficient of a resistor

of about 0.085mV/℃ at a desired inflection temperature T_{INF}, an amplifier gain of

K=2.35 would result in a zero temperature coefficient at T_{INF} [7].
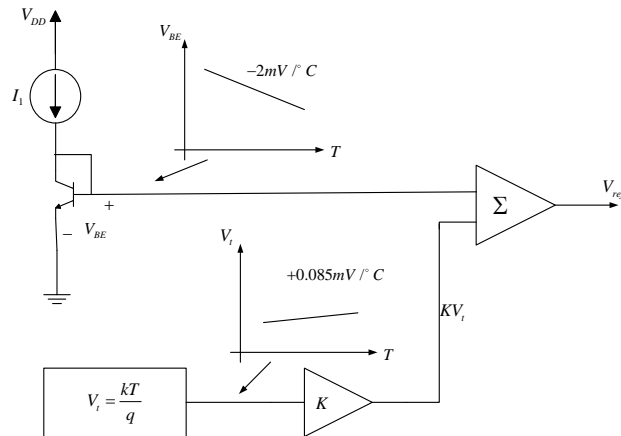
Figure 3 Basic structure of bandgap reference circuit

1.3 Variants of Bandgap Reference Circuits

There are several different bandgap reference circuits that have received considerable attention in the literature. Most bandgap circuits are based upon two observations. The first is that under constant current, the voltage across a PN junction has a negative temperature coefficient of around 2mV/°C. The second observation is that if the ratio of two diode currents is fixed, then the appropriate signed difference of the two diode voltages has a positive temperature. By appropriately weighting the sum, the temperature derivative will then vanish at a predetermined temperature. Even if the conditions listed for the two observations are not precisely satisfied, an appropriately weighted sum of a diode voltage and the difference of two diode voltages may still vanish at a predetermined temperature.
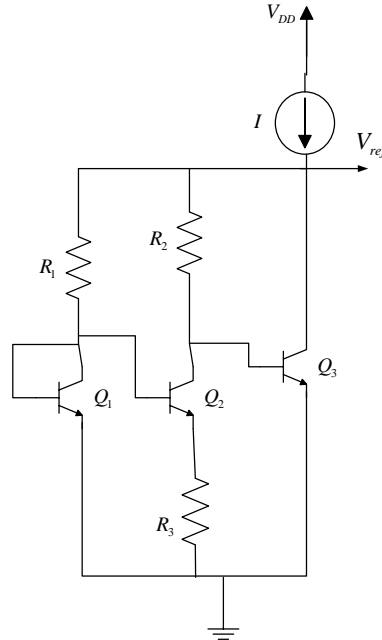
Figure 4 Widlar reference circuit

The Widlar circuit shown in Figure 4 is the earliest reported circuit voltage reference that has an output that is the weighted sum of a diode voltage and a difference of two diode voltages. In the Widlar structure, NPN transistors that have properties of

the base-emitter junction that are similar to those of a diode was used to build the reference. This structure uses the negative temperature coefficient of base-emitter voltage in conjunction with the positive temperature coefficient of difference of two base-emitter voltages operating at different current densities to make a zero temperature coefficient reference [5] at a predetermined temperature. Widlar reported that the reference voltage for this circuit can be expressed as:

$$V_{ref} = V_{g0}\left(1 - \frac{T}{T_0}\right) + V_{BE0}\left(\frac{T}{T_0}\right) + \frac{kT}{q}log_e\frac{J_1}{J_2} \tag{5}$$

Where $\frac{J_1}{J_2}$ is the ratio of the current densities of Q_1 and Q_2, $\frac{J_1}{J_2}$ is the temperature where the thermal derivative vanishes, $\frac{J_1}{J_2}$ is the bandgap voltage of silicon and $\frac{J_1}{J_2}$ is the base-emitter voltage of Q_3 at T_0 with collector current I_0.

Widlar than set the temperature derivative of the voltage in (5) to 0 at the inflection temperature T_0 to obtain the expression that must be satisfied to have a zero thermal derivative at T_0:

$$V_{g0} = V_{BE0} + \frac{kT_0}{q}log_e\frac{J_1}{J_2} \tag{6}$$

It is interesting to note that the Widlar analysis does not provide a closed-form expression for the output voltage of the circuit in terms of the model parameters of the devices.

Even though the Widlar reference circuit provides reasonably good performance, it still requires a relatively good current source that also presents design challenges.

The Brokaw reference circuit [6] shown in Figure 5 appeared shortly after the Widlar reference. Brokaw may have been the first author to use the term "bandgap". The Brokaw circuit still uses a combination of base-emitter voltages of BJT's but in

contrast to Widlar, Brokaw eliminated the fixed dc current source and eliminated one transistor. A regenerative feedback circuit was used to obtain low supply sensitivity. The regenerative feedback circuit also generates the bias currents for the two BJTs. The voltage at the base of Q_1 is the sum of the V_{be} of Q_1 and the voltage across R_1 which is proportional to the difference of the two base-emitter voltages. The resistor ratio, $\frac{R_1}{R_2}$, can be adjusted to change the relative weight of the base-emitter voltage and the difference of the two base-emitter voltages [6]. This structure is the first to use different areas of the PN junctions (actually different areas of the emitters of the BJTs) as a design variable. This structure has a rather large output voltage of about 2.5V and requires a correspondingly larger supply voltage to accommodate the operational amplifier. The Brokaw reference circuit is still used in industry.
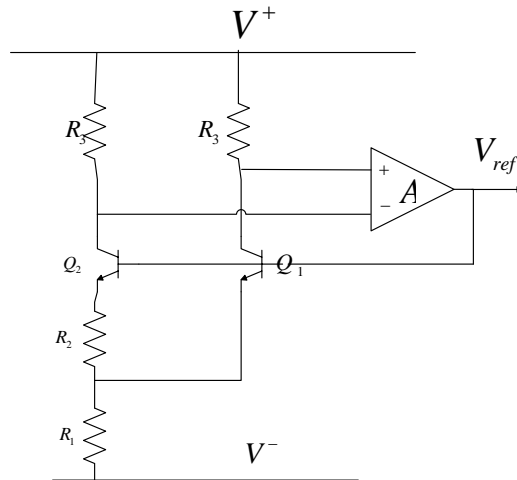
Figure 5 Brokaw reference circuit

There are many other bandgap circuits that have been proposed though the performance of most is not appreciably better than that of some of these earlier circuits. Two, in particular, will be discussed in this thesis. One is the Kujik circuit [8] which actually predates the Brokaw circuit and the other is the more recent Banba circuit [10]. These circuits will be discussed later.

1.4 Research Motivation

For many years, even though IC design engineers wanted to create new voltage reference structures with reduced temperature and supply sensitivity, lower supply voltages, lower power consumption, or with better trimming capabilities to enhance overall performance, there is little in the literature that suggests that they really looked deeply into the theory or fundamental operation of the bandgap reference circuits that had appeared in the literature. Though there are often comparisons of performance with existing structures presented by authors, these comparisons are often based upon either experimental results or computer simulations under somewhat varied conditions rather than based upon analytical formulations. Although such comparisons can be very useful, it remains difficult today to fairly compare or rank-order the performance of even some of the most basic structures bandgap reference structures. The challenges in making comparisons based upon experimental results or computer simulations can be attributable to several key factors. Several of these key factors will be identified. Firstly, most structures have several degrees of freedom in the design and how these degrees of freedom are used can affect the overall performance of a given circuit structure. The issue of how these degrees of freedom should be used to optimize the performance of a given structure is seldom discussed. The published results often involve substantially different process technologies. The temperature range over which measurements are made often differs. The number of samples used to obtain experimental results often differ significantly. The inflection point temperature is not consistent. The output voltage level varies. Methods used for the layout and placement

of critical components is seldom discussed. The method of calibration and number of

calibration points often differs. And some authors lump process variations and

temperature variations together whereas others separate these factors. As a result, there

are substantial differences in performance reported from one structure to another but it

is difficult to determine whether these differences are primarily attributable to

difference in architecture or differences in validation or reporting procedures.

Reported results are not void of some level of analytical formulation. Most

authors will discuss the first-order temperature coefficient of the reference voltage and

the goal of designing the circuit so that it vanishes at the inflection temperature point

but few if any actually obtain an analytical expression for V_{REF} that is only a function

of design and model parameters. Brokaw [6] did provide some comments about the

second-order temperature coefficient but not in terms of design and model parameters.

The Table 1 shows the equation of some widely used circuits and shows their

own performance the paper mentioned.

Table 1 Reference Equation of Bandgap Reference

Structures Name	Reference Voltage
Banba[10]	$V_{ref} = R_4(\frac{V_{diode}}{R_1} + \frac{V_T \ln(N)}{R_0})$ N ratio of the Diode2 to Diodes 1
Brokaw[6]	$V_{ref} = V_{G0} + \frac{T}{T_0}(V_{BE0} - V_{G0}) + (m-1)\frac{kT}{q}\ln\frac{T}{T_0} + (P_1+1)\frac{R_1}{R_2}\frac{kT}{q}\ln\frac{J_1}{J_2}$ P_1 emmitter current of $\frac{i_{e1}}{i_{e2}}$
Kuijk[8]	$V_{ref} = V_{G0} + (\eta-1)\frac{kT_0}{q} - \frac{1}{2}(\eta-1)\frac{kT_0}{q}(\frac{\Delta T}{T_0})^2$ η is equal to 4-n, n is the emission coefficient

Table 1 continued

Mietus[13]	$$V_{ref} = R_4(\frac{m\frac{kT}{q}\ln(x)}{R_0} + \frac{yV_{be}}{R_1})$$ m ratio of the current $\frac{I'_1}{I_1}$; x ratio of transistor emitter areas, $\frac{A_{34}}{A_{33}}$; y ratio of the current $\frac{I'_2}{I_2}$
Mixed BipolarMOS[15]	$$V_{ref} = (R_1 + R_2)\frac{mV_T \ln(L)}{R_1} + V_{CTAT}$$ m is inverse of the gate-to-surface coupling coefficient; L ratio of the diode-connected MOS

Table 2 Performance of several Reference Circuit

	Banba	Brokaw	Kuijik	Mietus	Mixed MOS-Bipolar
Output Voltage(V)	0.518	2.5	9.882	0.9	1.176
Temperature Range(℃)	98	180	60	70	120
Temperature Coefficient(ppm/℃)	591 include process variation	5 to 60 with laser trimming	4	nearly 0	12.75

In this work, a fair way of comparing the performance of these structures in a given process node from a temperature stability viewpoint will be presented. A metric for comparing not only the temperature characteristics of these structures but other bandgap references will be introduced. This comparison will be based upon an optimization of the design variables in each architecture.

CHAPTER II TRADITIOANL BANDGAP REFERENCE CIRCUIT

2.1 Diode and BJT Model

Since traditional bandgap reference circuits depend strongly upon the properties of a PN junction or the closely related diode-connected bipolar transistor, it is necessary to introduce the model for the diode and bipolar transistor that explicitly includes the dominant temperature dependence of these devices. Though there may be variants of the models for these devices that are different and possibly more accurate, the models presented in this section should be adequate for fairly comparing the performance of different bandgap reference circuits.

2.1.1 Diode Model

The model given in (7) is widely used to model the PN junction and will be used in this work. A sketch of the I-V characteristics is shown in Figure 6 for a typical set of process parameters.

$$I = I_s \left(e^{\frac{V}{nV_T}} - 1 \right) \tag{7}$$

In this equation:

I_s = saturation current

I = diode current

V = is the voltage from anode to cathode

V_T = thermal voltage

n = emission coefficient
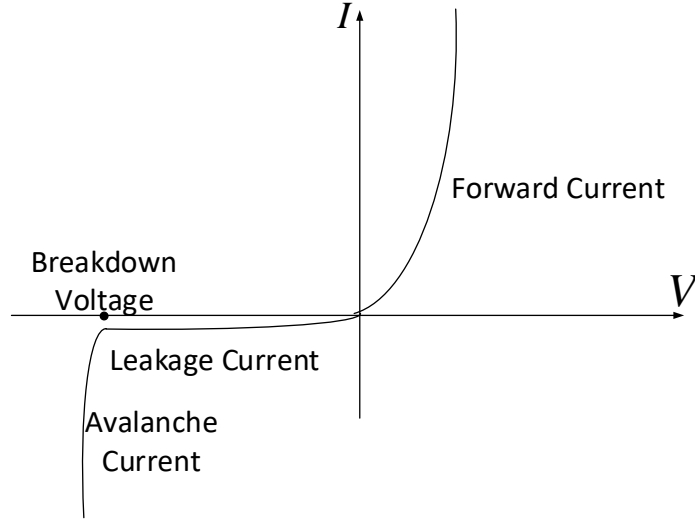
Figure 6 I-V characteristics of a diode

Since we are interested in the thermal characteristics of a bandgap reference, it is necessary to identify the temperature dependent terms in (7). In addition to the thermal voltage, the parameter I_S is highly dependent. The saturation current I_S can be expressed as:

$$I_s = J_S A e^{-\frac{V_{G0}}{V_T}} \tag{8}$$

Where A is the junction area of the diode, J_S is the transport saturation current density [11], and V_{G0} is the bandgap voltage of the silicon V_{G0} is a generally considered to be a physical constant thought it has a very weak dependence on temperature which will be ignored here. The bandgap voltage of silicon is about 1.2V.

The parameter J_S is also highly temperature dependent and can be expressed as:

$$J_S = \frac{q D_p n_i^2}{L_p N_D} + \frac{q D_n n_i^2}{L_n N_A} \tag{9}$$

Where q is the charge of an electron, $D_{n,p}$ are diffusion coefficient of holes and electrons, respectively; n_i is the intrinsic carrier concentration in silicon; $N_{D,A}$

are donor and acceptor concentrations at the n side and p side, respectively; $L_{p,n}$ are

the diffusion length at the n side and p side, respectively.

Normally, the n_i is assumed to have some temperature dependence and the

parameter n_i can be expressed as:

$$n_i \approx kT^t \tag{10}$$

In the equation (10), k is a constant value versus temperature and the exponent

t is typically around 1.5.

The diffusion length can be expressed like this:

$$L_p = \sqrt{D_p \tau_p} \tag{11}$$

τ_p is the carrier lifetimes of holes. Moreover, the component $\dfrac{D_p}{\tau_p}$ is

proportional to T^γ and γ is a constant value.

For the equation (9) only the first part of the (9) would be considered, since the second

part will behave similarly to the first one, then

$$J_s \approx \frac{q D_p n_i^2}{L_p N_D} \approx q \sqrt{\frac{D_p}{\tau_p}} \frac{n_i^2}{N_D} \propto T^{(3+\frac{\gamma}{2})} e^{-\frac{V_{G0}}{nkT}} \tag{12}$$

Even though, for more accurate analysis, there is still other parameters that has

temperature dependent like γ and the T^3 is not the only one temperature component

for the J_s, the Spice simulator default set the temperature coefficient to three to simplify

the equation there. For convenient analysis, this saturation current temperature

exponent is expressed with m, since this parameter would vary according to different

situation and analysis. The saturation current can be expressed like this:

$$I_s = J_{s0} T^m A e^{-\frac{V_{G0}}{nV_T}} \tag{13}$$

In this equation, J_{s0} can be regards as temperature-independent process parameter that represents the constant component of J_s. Combining these results into a single equation, it follows that the diode current versus temperature and voltage can be expressed as:

$$I = I_s \left(e^{\frac{V}{nV_T}} - 1 \right) = J_{s0} T^m A e^{-\frac{V_{G0}}{nV_T}} (e^{\frac{V}{nV_T}} - 1) \tag{14}$$

In applications of the diode discussed in this work, the diode will be operating in the saturation region where normally the component, $e^{\frac{V}{nV_T}}$, is much larger than one. Thus the diode model equation (14) can be written as:

$$I = J_{s0} T^m A e^{\frac{V - V_G}{nV_T}} \tag{15}$$

2.1.2 BJT Model

The model for the bipolar transistor is really close to that of the diode but there are slightly differences. In what follows, an analytical model for the BJT will be given.

The starting point will be the dc model introduced by Ebers and Moll in the 1954 [12]. In this model the relationship between the terminal variables is given by:

$$I_C = I_S \left(e^{\frac{V_{BE}}{V_T}} - 1 \right) - \frac{I_S}{\alpha_R} (e^{\frac{V_{BC}}{V_T}} - 1) \tag{16}$$

$$I_E = -\frac{I_S}{\alpha_F} \left(e^{\frac{V_{BE}}{V_T}} - 1 \right) + I_S (e^{\frac{V_{BC}}{V_T}} - 1) \tag{17}$$

In the equation above, I_S is the transport saturation current, α_R is the reverse current gain of common base configuration and α_F is the forward current gain of common base configuration.

In the designs that are discussed in this thesis the reverse current can be neglected and in the bandgap reference circuits, the critical current that flows in a resistor to generate the positive temperature coefficient voltage is the collector current,

the forward collector current is the main focus. It follows from (16) and (17) that the collector current can be expressed as:

$$I_C = I_S \left(e^{\frac{V_{BE}}{V_T}} - 1 \right) \tag{18}$$

Normally, the forward emission current coefficient may not be equal to one. Including the emission coefficient, n, in the model equation it follows that:

$$I_C = I_S \left(e^{\frac{V_{BE}}{nV_T}} - 1 \right) \tag{19}$$

The parameter I_S has the same temperature dependence as the corresponding parameter for the diode. Thus, it follows by substituting from equation (13) into equation (19) that the collector current can be expressed as

$$I_C = I_S \left(e^{\frac{V}{nV_T}} - 1 \right) = J_{s0} T^3 A e^{-\frac{V_G}{nV_T}} (e^{\frac{V}{nV_T}} - 1) \tag{20}$$

For the bipolar transistor, the parameter A is the emitter area. For the same reason as given for the diode, if the bipolar transistor operates in the forward active region, the $e^{\frac{V}{nV_T}}$ term is much larger than one so the component '1' can neglected. The current can thus be expressed as:

$$I_C = I_S \left(e^{\frac{V}{nV_T}} - 1 \right) = J_{s0} T^m A e^{-\frac{V_G}{nV_T}} e^{\frac{V}{nV_T}} = J_{s0} T^m A e^{\frac{V-V_G}{nV_T}} \tag{21}$$

2.2 Brokaw Reference Circuit

The circuit shown in Figure 7 which was designed in a bipolar process is a popular bandgap circuit that has been around since the mid 1970's [6] and is still widely used today in bipolar processes. This circuit will now be analyzed with the goal of obtaining an explicit expression for the output voltage in terms of only model parameters and design variables. From the explicit expression, an explicit expression for the temperature dependence of the output will be obtained.
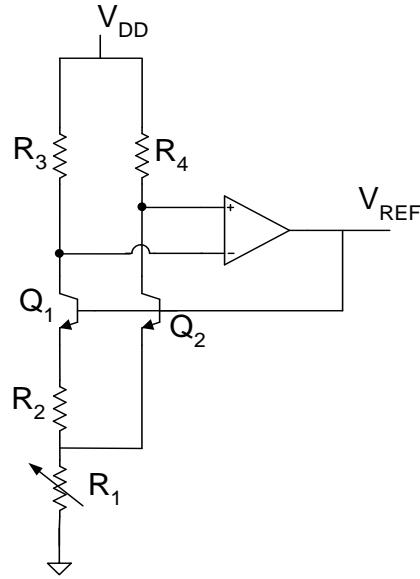
Figure 7 Standard Brokaw reference circuit structure

In this circuit, the resistor values for R_3 and R_4 are often set the same to make the collector currents of the two branches the same. The emitter current that flows through the bipolar transistor Q_1 is designated as I_1 and the emitter current the flows through the bipolar transistor Q_2 is designated as I_2. If the two resistors R_3 and R_4 are the same and if the β of both transistors are large so that the base current can be neglected, it follows that:

$$I_1 = I_2 \tag{22}$$

The relationship between V_{BE1}, V_{BE2} and I_1 can be expressed as:

$$V_{BE1} + I_1 R_2 = V_{BE2} \tag{23}$$

The reference voltage can be expressed as:

$$V_{ref} = V_{BE2} + (I_1 + I_2)R_1 \tag{24}$$

Since the collector and emitter currents are assumed to be the same, it follows from equation (19), the V_{BE1} and V_{BE2} can be expressed like this:

$$V_{BE1} = nV_T \ln\left(\frac{I_1}{I_{s1}}\right) \tag{25}$$

$$V_{BE2} = nV_T \ln\left(\frac{I_2}{I_{s2}}\right) \tag{26}$$

The five independent equations (22), (23), (24), (25) and (26) comprise a complete set of equations in the unknowns $\{I_1, I_2, V_{BE1}, V_{BE2}, V_{REF}\}$ and can be solved for any of these unknowns.

From the equations (25) and (26), it is easy to calculate the difference of the base-emitter voltage of two bipolar:

$$V_{BE2} - V_{BE1} = V_T \ln\left(\frac{I_1}{I_{s1}}\frac{I_{s2}}{I_2}\right) \tag{27}$$

And from the equation (13), assuming the devices are in the same process so that $J_{S01}=J_{S02}=J_{S0}$, the saturation currents can be expressed:

$$\left.\begin{array}{l} I_{s1} = J_{s0}T^m A_1 e^{-\frac{V_{G0}}{nV_T}} \\ I_{s2} = J_{s0}T^m A_2 e^{-\frac{V_{G0}}{nV_T}} \end{array}\right\} \tag{28}$$

The reference voltage given in equation (24) is made up of two parts, one is V_{BE2} that is the CTAT and the other is the voltage across the R_1 which is PTAT. Since $I_1=I_2$ it follows that the PTAT voltage is:

$$V_{PTAT} = (I_1 + I_2)R_1 = 2I_1 R_1 \tag{29}$$

Substituting from (23) and (27) into (29), the PTAT voltage can be expressed as:

$$V_{PTAT} = 2\frac{V_{BE2}-V_{BE1}}{R_2}R_1 = 2nV_T \ln\left(\frac{A_2}{A_1}\right)\frac{R_1}{R_2} = 2\,n\ln\left(\frac{A_2}{A_1}\right)\frac{kR_1}{qR_2}T \tag{30}$$

For CTAT voltage, it is just determined by the V_{BE2}.

$$V_{CTAT} = V_{BE2} = nV_t \ln\left(\frac{I_2}{I_{s2}}\right) \tag{31}$$

The current I_2 can be expressed as:

$$I_2 = I_1 = \frac{V_{BE2}-V_{BE1}}{R_2} = V_T \ln\left(\frac{I_1}{I_{s1}}\frac{I_{s2}}{I_2}\right) = n\ln\left(\frac{A_2}{A_1}\right)\frac{k}{qR_2}T \tag{32}$$

Substituting the equation (28) and (32) back into equation (31) to get the equation (33):

$$V_{CTAT} = nV_t \ln\left(\frac{I_2}{I_{s2}}\right) = n\frac{kT}{q}\ln\left(n\ln\left(\frac{A_2}{A_1}\right)\frac{k}{qR_2}T\right) - n\frac{kT}{q}\ln(J_{s0}T^3 A_2 e^{-\frac{V_{G0}}{nkT}}) \quad (33)$$

Substituting equations (30) and (31) back into equation (24), V_{ref} can be expressed like this:

$$V_{ref} = V_{G0} + \frac{n}{kq}\left(n\ln\left(\ln\left(\frac{A_2}{A_1}\right)\frac{k}{qR_2}\right) + \ln\left(\frac{A_2}{A_1}\right)\frac{R_1}{R_2}\right)T - (m-1)n\frac{k}{q}TlnT \quad (34)$$

This is a closed-form explicit expression that also explicitly shows the temperature dependence. The temperature dependence if of the form:

$$V_{ref} = a + bT + cTlnT \quad (35)$$

where the terms a, b and c are independent of temperature. In the Brokaw reference circuit, these parameters are respectively:

$$\left.\begin{array}{c} a = V_{G0} \\ b = \frac{n}{kq}\left(n\ln\left(\ln\left(\frac{A_2}{A_1}\right)\frac{k}{qR_2}\right) + \ln\left(\frac{A_2}{A_1}\right)\frac{R_1}{R_2}\right) \\ c = -(m-1)n\frac{k}{q} \end{array}\right\} \quad (36)$$

The reference voltage of the Brokaw circuit is comprised of the sum of a constant term, a, a first-order term with coefficient b, and a higher-order term with coefficient c. The Brokaw circuit is comprised of three design variables, {A_2/A_1, R_2, R_1/R_2}. The terms a and c are independent of the design variables and the coefficient b is a rather complicated function of the design variables.

2.3 Banba Reference Circuit

The Banba reference [10] circuit showed in the Figure 8 was proposed for use in a MOS process rather than the bipolar used for the Brokaw reference circuit. In

standard MOS processes, a good bipolar transistor is generally not available. As an alternative, the Banba circuit uses PN junctions instead to create diodes and correspondingly the PTAT and CTAT voltages similar to those generated by Brokaw. Even good PN junctions are not available in standard MOS processes so diode-connected substrate PNP transistors are typically used to create the diodes. One of the salient features of the Banba reference is operation at lower supply voltages with low power consumption.

Figure 8 Standard Banba reference circuit

For the Banba circuit, analysis is similar to that of the Brokaw circuit. It also uses an Opamp to balance the voltage of two nodes. The current flow in the diodes, D_1 and D_2, are I_{D1} and I_{D2} respectively. The current flow in the resistors R_1 and R_2 are I_{R1} and I_{R2}. For convenience, the transistors, M_1, M_2 and M_3 are sized the same and the resistor R_1 and R_2 are assumed to have the same value.

From basic circuit analysis, the five independent equations in (37) can be readily obtained. There are five unknowns in these equations; {I_{D1}, I_{D2}, V_{D2}, V_{D1}, V_{REF}}

$$V_{D1} = V_{D2} + I_{D2}R_0$$
$$I_{D1} = I_{D2}$$
$$I_{D1} = J_{s0}A_1 T^m e^{\left(\frac{V_{D1}-V_{G0}}{n\frac{kT}{q}}\right)}$$
$$I_{D2} = J_{s0}A_2 T^m e^{\left(\frac{V_{D2}-V_{G0}}{n\frac{kT}{q}}\right)}$$
$$V_{ref} = R_3\left(\frac{V_{D1}}{R_1} + I_{D1}\right)$$

$$(37)$$

With tedious manipulations, these equations can be solved to obtain an expression for the reference voltage which can be written as:

$$V_{ref} = \frac{R_3}{R_1}V_{G0} + n\frac{kR_3}{qR_1}\left(\ln\left(n\ln\left(\frac{A_2}{A_1}\right)\frac{k}{qR_2 J_{s0}}\right) + \ln\left(\frac{A_2}{A_1}\right)\frac{R_3}{R_0}\right)T - (m-1)n\frac{kR_3}{qR_1}T\ln T \quad (38)$$

Equation (38) can be expressed in the same format as equation (35) where the parameters a, b and c are given by:

$$\begin{cases} a = \frac{R_3}{R_1}V_{G0} \\ b = n\frac{kR_3}{qR_1}\left(\ln\left(n\ln\left(\frac{A_2}{A_1}\right)\frac{k}{qR_2 J_{s0}}\right) + \ln\left(\frac{A_2}{A_1}\right)\frac{R_3}{R_0}\right) \\ c = -(m-1)n\frac{kR_3}{qR_1} \end{cases} \quad (39)$$

The parameter b seems to be very complicated and includes the four remaining design variables $\{R_3/R_1, A_2/A_1, R_3/R_0, R_2\}$. Note the parameter b in this circuit is different from the parameter b of the Brokaw circuit.

2.4 Kuijk Reference Circuit

Another basic bandgap circuit is shown in Figure 9. This circuit was first discussed by Kuijk in 1973 [8]. Kuijk used diode-connected transistors and we are simply using diodes in our implementation. It is similar to the Banba circuit but uses resistors to supply the current to the diodes. This structure seems simpler than the previous two.
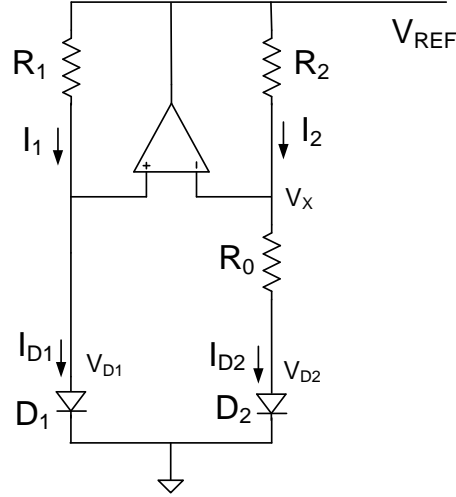
Figure 9 Standard Kuijk Reference Circuit

Its analysis is very similar to that of the other two as well. For convenience, it will be assumed that $R_1=R_2$. If follows from a basic circuit analysis that the following five equations are independent with the five unknowns $\{I_{D1}, I_{D2}, V_{D1}, V_{D2}, V_{REF}\}$.

$$\left.\begin{array}{l} I_{D2} = \dfrac{V_{D1} - V_{D2}}{R_0} \\[2mm] I_{D1} = I_{D2} \\[2mm] I_{D1} = J_{S0}A_1 T^m e^{\frac{V_{D1}-V_{G0}}{n\frac{kT}{q}}} \\[2mm] I_{D2} = J_{S0}A_2 T^m e^{\frac{V_{D2}-V_{G0}}{n\frac{kT}{q}}} \\[2mm] V_{REF} = V_{D1} + I_{D2}R_2 \end{array}\right\} \qquad (40)$$

After some tedious manipulations of the equations in (40), the reference voltage can be expressed like this:

$$V_{ref} = V_{G0} + n\frac{k}{q}\left(\ln\left(n\ln\left(\tfrac{A_2}{A_1}\right)\tfrac{k}{qR_0 J_{s0}}\right) - \ln\left(\tfrac{A_2}{A_1}\right)\tfrac{1}{R_0}\right)T - (m-1)n\frac{k}{q}T\ln T \quad (41)$$

As with the Brokaw and Banba reference circuits, this structure has the same format as equation (35) where the parameters a, b and c are given by:

$$\begin{cases} a = V_{G0} \\[2mm] b = n\dfrac{k}{q}\left(\ln\left(n\ln\left(\tfrac{A_2}{A_1}\right)\tfrac{k}{qR_0 J_{s0}}\right) - \ln\left(\tfrac{A_2}{A_1}\right)\tfrac{1}{R_0}\right) \\[2mm] c = -(m-1)n\dfrac{k}{q} \end{cases} \qquad (42)$$

In this structure, the expression for the parameter b is still complex and characterized by the design variables $\{A_2/A_1, R_0\}$.

2.5 Mietus Reference Circuit

There is another popular structure that is published in 1997 by Mietus[13]. The structure is shown in Figure 10.
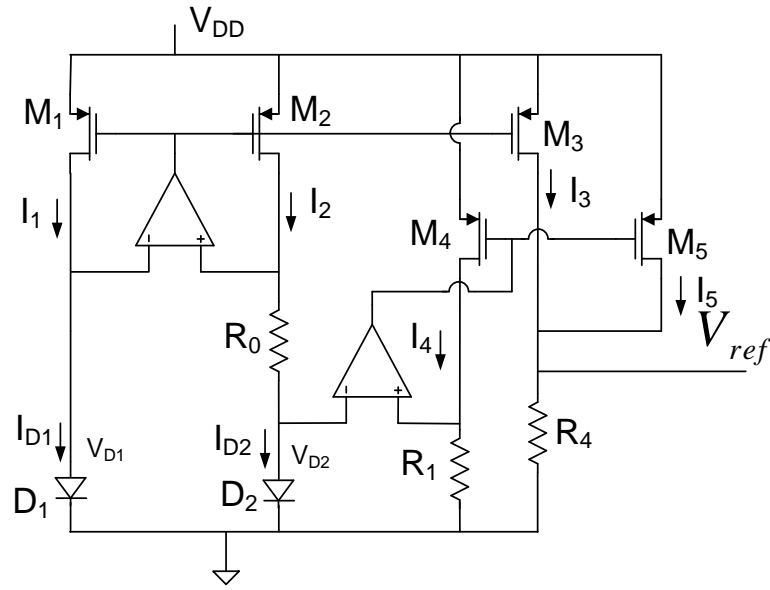
Figure 10 Low Voltage Reference of Mietus

Even though the structure seems a little bit more complex than the previous three, the actual analysis is similar: If follows from a basic circuit analysis that the following eight equations are independent with the eight unknowns $\{I_{D1}, I_{D2}, I_3, I_4, I_5, V_{D1}, V_{D2}, V_{REF}\}$ where the design variables K_1, K_2, and K_5 represent mirror gains.

$$
\left.
\begin{aligned}
I_{D2} &= \frac{V_{D1} - V_{D2}}{R_0} \\
I_{D1} &= K_1 I_{D2} \\
I_3 &= K_3 I_{D2} \\
I_5 &= K_5 I_4 \\
I_4 &= \frac{V_{D2}}{R_1} \\
I_{D1} &= J_{S0} A_1 T^m e^{\frac{V_{D1} - V_{G0}}{n\frac{kT}{q}}} \\
I_{D2} &= J_{S0} A_2 T^m e^{\frac{V_{D2} - V_{G0}}{n\frac{kT}{q}}} \\
V_{REF} &= \left(I_3 + I_5\right) R_4
\end{aligned}
\right\}
\tag{43}
$$

After some tedious manipulation of the equation set of (43), the reference voltage can be expressed like this:

$$V_{ref} = K_5 V_{G0} + n\frac{k}{q}\left(K_3\frac{R_4}{R_0}\ln\left(K_1\frac{A_{D2}}{A_{D1}}\right) + K_5\left(ln\frac{k}{q} + \frac{\ln\left(K_1\frac{A_{D2}}{A_{D1}}\right)}{J_{s0}A_{D2}}\right)\right)T - (m-1)nK_5\frac{k}{q}TlnT \quad (44)$$

This structure has a V_{ref} that is of the same format as equation (35) where the parameters a, b and c are given by:

$$\left.\begin{array}{c} a = K_5 V_{G0} \\ b = n\frac{k}{q}\left(K_3\frac{R_4}{R_0}\ln\left(K_1\frac{A_{D2}}{A_{D1}}\right) + K_5\left(ln\frac{k}{q} + \frac{\ln\left(K_1\frac{A_{D2}}{A_{D1}}\right)}{J_{s0}A_{D2}}\right)\right) \\ c = -(m-1)nK_5\frac{k}{q} \end{array}\right\} \quad (45)$$

From the equation (45), the parameter b of the Mietus structure is even more complicated and includes the six design variables $\{K_1, K_3, K_5, R_4/R_0, A_{D2}/A_{D1}, A_{D2}\}$. In contrast to the other structures, the parameters a and c also include the design variable K_5.

2.6 Mixed Bipolar-MOS Reference Circuit

This sructure shown in the Figure 11 [15] s significantly different than the other four discussed above since it contains only a single diode and an array of MOS transistors that are operating in weak inversion. The transistors $M_{21}...M_{2L}$ are assumed to be sized the same.
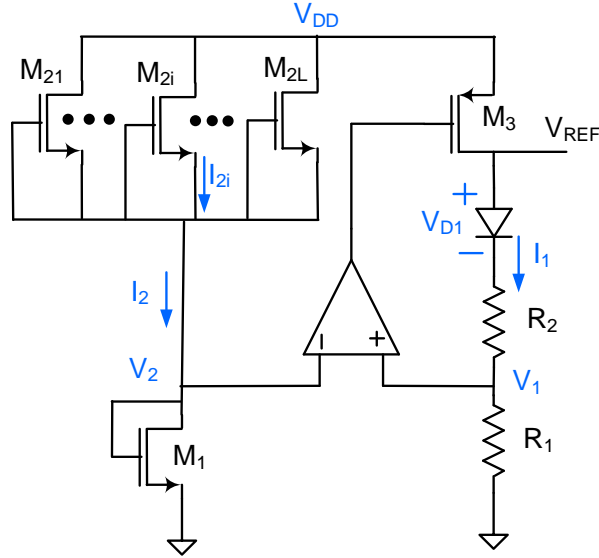
Figure 11 Mixed Bipolar-MOS Reference Structure

The weak inversion model of the drain current of the n-channel and p-channel MOS transistors, assumed to be operating in weak-inversion saturation, are given respectively by the expressions:

$$I_{nch} = \frac{W_n}{L_n} \frac{2\mu_n C_{OX}}{e^2} \left(n_{wn} \frac{kT}{q} \right)^2 e^{\frac{V_{GS} - V_{THn}}{n_{wn} V_t}}$$

$$I_{pch} = -\frac{W_p}{L_p} \frac{2\mu_p C_{OX}}{e^2} \left(n_{wp} \frac{kT}{q} \right)^2 e^{-\frac{V_{GS} - V_{THp}}{n_{wp} V_t}} \tag{46}$$

where n_{wn} and n_{wp} are the weak-inversion emission coefficients, where V_{THn} and V_{THn} are the threshold voltages of the n-channel and the p-channel transistors, and where Vt=kT/q.

From a basic circuit analysis, the following set of five equations in the unknowns {I₁, I₂, V_{D1}, V₂, V_{REF}} can be obtained. In these equations, (47), n_L is the number of parallel transistors in the upper-left array.

$$I_2 = n_L \frac{W_2}{L_2} \frac{2\mu_n C_{OX}}{e^2} \left(n_{wn} \frac{kT}{q} \right)^2 e^{\frac{-V_{THn}}{n_{wn}V_t}}$$

$$I_2 = \frac{W_1}{L_1} \frac{2\mu_n C_{OX}}{e^2} \left(n_{wn} \frac{kT}{q} \right)^2 e^{\frac{V_2 - V_{THn}}{n_{wn}V_t}}$$

$$I_1 = \frac{V_2}{R_1}$$

$$I_1 = J_{S0} A_D T^m e^{n\frac{V_{D1}-V_{G0}}{\frac{kT}{q}}}$$

$$V_{REF} = I_1 (R_1 + R_2)$$

(47)

After some tedious manipulations, an expression for the reference voltage can

be obtained and expressed like this:

$$V_{ref} = V_{G0} + \left[\frac{k}{q}(R_1 + R_2) * \frac{m\ln(L)}{R_1} + \frac{k}{q}n\ln\left(\frac{m\ln(L)k}{qR_1 J_{S0} A_{D1}}\right)\right] * T - (m-1)\frac{k}{q}nTlnT \quad (48)$$

This structure has a V_{ref} that is of the same format as equation (35) where the

parameters a, b and c are given by:

$$a = V_{G0}$$
$$b = \left[\frac{k}{q}(R_1 + R_2) * \frac{m\ln(L)}{R_1} + \frac{k}{q}n\ln\left(\frac{m\ln(L)k}{qR_1 J_{S0} A_{D1}}\right)\right]$$
$$c = -(m-1)n\frac{k}{q}$$

(49)

The parameter b includes the four design variables $\{R_1, R_2, L, A_{D1}\}$.

2.7 Alternate Banba Refrence Circuit

The original Banba reference circuit includes a large number of devices and

several design degrees of freedom. A simplified version of the Banba circuit appears in

Figure 12. It will be assumed for convenience that the size of M_1, M_2 and M_3 are the

same and the size of M_4 and M_5 are the same.
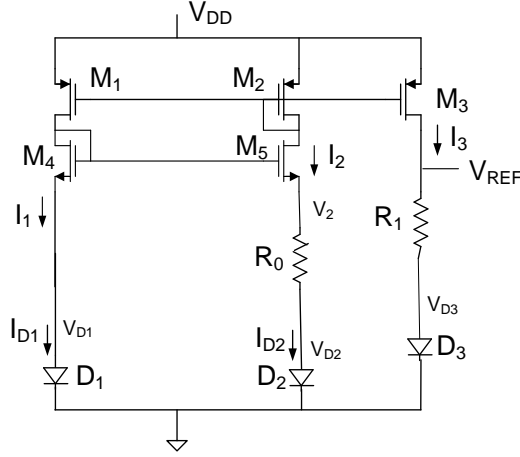
Figure 12 Modified Banba Reference Structure

If the output impedance of the MOS transistors assumed is assumed to be infinite, it follows from a basic circuit analysis that the eight equations in equation group (50) are independent in the eight unknowns {I_{D1}, I_{D2}, I_{D3}, V_2, V_{D1}, V_{D2}, V_{D3}, V_{REF}}.

$$
\left.
\begin{aligned}
I_2 &= L\frac{W_2}{L_2}\frac{2\mu C_{OX}}{e^2}\left(n\frac{kT}{q}\right)^2 e^{\frac{-V_{TH}}{nV_t}} \\
I_2 &= \frac{W_1}{L_1}\frac{2\mu C_{OX}}{e^2}\left(n\frac{kT}{q}\right)^2 e^{\frac{V_2-V_{TH}}{nV_t}} \\
I_1 &= \frac{V_2}{R_1} \\
I_1 &= J_{S0}A_D T^m e^{\frac{V_{D1}-V_{G0}}{n\frac{kT}{q}}} \\
V_{REF} &= I_1\left(R_1+R_2\right)
\end{aligned}
\right\}
\qquad (50)
$$

After some tedious manipulations of these equations, an explicit expression for V_{REF} can be obtained which can be expressed like this:

$$
V_{ref} = V_{G0} + n\frac{k}{q}\left(\ln\left(\frac{A_{D1}}{A_{D3}}\frac{k}{q}\frac{\ln\left(\frac{A_{D2}}{A_{D1}}\right)}{J_{S0}A_{D1}R_0}\right)T + \frac{R_1}{R_0}\ln\left(\frac{A_{D2}}{A_{D1}}\right)\right)T - (m-1)n\frac{k}{q}T\ln T \quad (51)
$$

This is of the same form as equation (35) where the parameter a, b and c respectively are:

$$a = V_{G0}$$

$$b = n\frac{k}{q}\left(\ln\left(\frac{A_{D1}}{A_{D3}}\frac{k}{q}\frac{\ln\left(\frac{A_{D2}}{A_{D1}}\right)}{J_{S0}A_{D1}R_0} \right)T + \frac{R_1}{R_0}\ln\left(\frac{A_{D2}}{A_{D1}} \right) \right)$$

$$c = -(m-1)n\frac{k}{q}$$

$$\left.\begin{array}{c}\\\\\\\end{array}\right\} \quad (52)$$

As observed for the other circuits considered, the expression for a and c are

independent of design variables and the complicated coefficient b is a function of the

five design variables $\{A_{D1}/A_{D3}, A_{D1}/A_{D2}, A_{D1}, R_0, R_1/R_0\}$.

2.8 Modified Kuijk Reference Circuit

The modified Kuijk reference circuit shown in Figure 13 can be used to reduce

the power supply sensitivity. For convenience, the size of R_1 and R_2, will be assumed

to be the same.
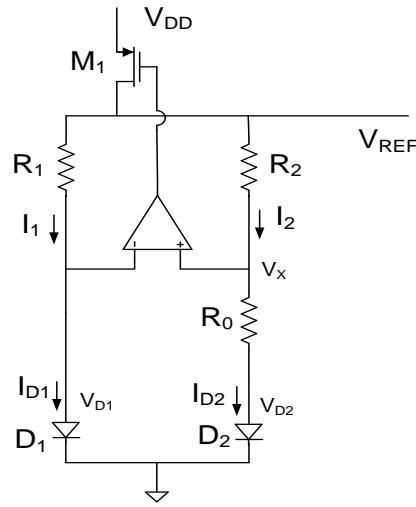
Figure 13 Modified Kuijk Reference Circuit Structure

It follows from a basic circuit analysis that the five equations in equation group

(53) are independent in the five unknowns $\{I_{D1}, I_{D2}, V_{D1}, V_{D2}, V_{REF}\}$.

$$I_{D2} = \frac{V_{D1} - V_{D2}}{R_0}$$

$$I_{D1} = I_{D2}$$

$$I_{D1} = J_{S0}A_1 T^m e^{\frac{V_{D1}-V_{G0}}{n\frac{kT}{q}}}$$

$$I_{D2} = J_{S0}A_2 T^m e^{\frac{V_{D2}-V_{G0}}{n\frac{kT}{q}}}$$

$$V_{REF} = V_{D1} + I_{D2}R_2$$

$$\left.\begin{array}{c}\\\\\\\\\\\end{array}\right\} \quad (53)$$

This is identical to the equation set obtained for the original Kujik circuit so the solution will be the same as well. Thus, V_{REF} can be expressed as:

$$V_{REF} = V_{G0} + n\frac{k}{q}\left(\frac{R_2}{R_0}\ln\left(\frac{R_2}{R_1}\frac{A_{D2}}{A_{D1}}\right) + \ln\left(\frac{R_2}{R_1}\frac{k}{q}\frac{\ln\left(\frac{R_2 A_{D2}}{R_1 A_{D1}}\right)}{R_0 A_{D1} J_{S0}}\right)\right)T - (m-1)n\frac{k}{q}TlnT \quad (54)$$

This has the same form as equation (35) where the parameters a, b, and c of the modified Kuijk circuit are:

$$\left.\begin{aligned} a &= nV_{G0} \\ b &= n\frac{k}{q}\left(\frac{R_2}{R_0}\ln\left(\frac{R_2}{R_1}\frac{A_{D2}}{A_{D1}}\right) + \ln\left(\frac{R_2}{R_1}\frac{k}{q}\frac{\ln\left(\frac{R_2 A_{D2}}{R_1 A_{D1}}\right)}{R_0 A_{D1} J_{S0}}\right)\right) \\ c &= -(m-1)n\frac{k}{q} \end{aligned}\right\} \quad (55)$$

This could have been anticipated without repeating the analysis since the combination of the OpAmp and transistor M_1 could be viewed as a different OpAmp.

2.9 Summarized parameters of each structure

The structure discussed above all have the explicit dependent on temperature as given in equation (35) and the temperature dependence under normal operation is characterized by the parameters a, b and c for each structure. The parameters a, b and c for each structure are compiled in Table 3. As observed previously, the expressions for parameter b are quite complex for each structure but the expressions for the parameters a and c are simple, similar, and most are independent of any design variables.

Table 3 Summary of parameter of each structure

Structure Name	a	b	c	DoF
Brokaw	V_{G0}	$\frac{nk}{q}\left(n\ln\left(\ln\left(\frac{A_2}{A_1}\right)\frac{k}{qR_2}\right) + \ln\left(\frac{A_2}{A_1}\right)\frac{R_1}{R_2}\right)$	$-(m-1)n\frac{k}{q}$	3
Banba	$\frac{R_3}{R_1}V_{G0}$	$n\frac{kR_3}{qR_1}\left(\ln\left(n\ln\left(\frac{A_2}{A_1}\right)\frac{k}{qR_2 J_{s0}}\right) + \ln\left(\frac{A_2}{A_1}\right)\frac{R_3}{R_0}\right)$	$-(m-1)n\frac{R_3}{R_1}\frac{k}{q}$	4

Table 3 continued

Structure Name	a	b	c	DoF
Kuijk	V_{G0}	$n\frac{k}{q}\left(\ln\left(n\ln\left(\frac{A_2}{A_1}\right)\frac{k}{qR_0J_{s0}}\right)-\ln\left(\frac{A_2}{A_1}\right)\frac{1}{R_0}\right)$	$-(m-1)n\dfrac{k}{q}$	2
Mietus	V_{G0}	$n\frac{k}{q}\left(K_3\frac{R_4}{R_0}\ln\left(K_1\frac{A_{D2}}{A_{D1}}\right)+K_5\left(ln\frac{k}{q}+\frac{\ln\left(K_1\frac{A_{D2}}{A_{D1}}\right)}{J_{s0}A_{D2}}\right)\right)$	$-(m-1)n\dfrac{k}{q}$	6
Mixed Bio-MOS	V_{G0}	$\left[\frac{k}{q}(R_1+R_2)*\frac{m\ln(L)}{R_1}+\frac{k}{q}n\ln\left(\frac{m\ln(L)k}{qR_1J_{s0}A_{D1}}\right)\right]$	$-(m-1)n\dfrac{k}{q}$	4
Alternated Banba	V_{G0}	$n\frac{k}{q}\left(\ln\left(\frac{A_{D1}}{A_{D3}}\frac{k}{q}\frac{\ln\left(\frac{A_{D2}}{A_{D1}}\right)}{J_{s0}A_{D1}R_0}\right)T+\frac{R_1}{R_0}\ln\left(\frac{A_{D2}}{A_{D1}}\right)\right)$	$-(m-1)n\dfrac{k}{q}$	5
Modified Kuijk	V_{G0}	$n\frac{k}{q}\left(n\frac{R_2}{R_0}\ln\left(\frac{R_2}{R_1}\frac{A_{D2}}{A_{D1}}\right)+\ln\left(\frac{R_2}{R_1}\frac{k}{q}\frac{\ln\left(\frac{R_2}{R_1}\frac{A_{D2}}{A_{D1}}\right)}{R_0A_{D1}J_{s0}}\right)\right)$	$-(m-1)n\dfrac{k}{q}$	2

Considering the significant differences in the expressions for b and the number of different design variables that comprise b, it appears to be difficult to objectively and fairly compare the relative temperature performance of these different circuits. In what follows, a fair and objective comparison of the temperature characteristics of these circuits will be made.

CHAPTER III CHARACTERIZATION AND COMPARISON OF BANDGAP CIRCUITS

Normally, the first step in building a reference circuit is to force the first-order derivative to vanish at the desired temperature which here will be referred to as the inflection point temperature, T_{INF}. This can be stated mathematically as forcing:

$$\left.\frac{\partial V_{REF}(T)}{\partial T}\right|_{T=T_{INF}} = 0 \qquad (56)$$

This requires using at least one of the design variables to set T_{INF}. Equation (56) represents a constraint. If the expression for $V_{REF}(T)$ has n degrees of freedom, setting the constraint reduces the number of remaining degrees of freedom to n-1 and these can be used to achieve other desirable goals in the circuit. In the context of the bandgap references that have an output voltage of the form given in (35) and repeated as (57):

$$V_{REF}(T) = a + bT + cT\ln T \qquad (57)$$

where a, b and c are independent of temperature, the constraint equation becomes:

$$b + c(1 + \ln T)\big|_{T=T_{INF}} = 0 \qquad (58)$$

This constraint equation can be equivalently expressed as

$$T_{INF} = e^{-\left(1+\frac{b}{c}\right)} \qquad (59)$$

However, all references that are included in the comparison group selected in this thesis will be designed to satisfy the constraint so satisfying this constraint equation has nothing to do with the relative performance.

3.1 Temperature Coefficients with Vanishing Temperature Derivative at T_{INF}

Imagine different transfer characteristics of circuits that all satisfy the inflection point constraint such as those shown in Figure 14. Some are concave upward and some are concave downward. And some have a large curvature at the inflection temperature and others have a small curvature at the inflection temperature. In this depiction, T_{INF} is at 300K or equivalently at 27°C which is normally considered to be room temperature.
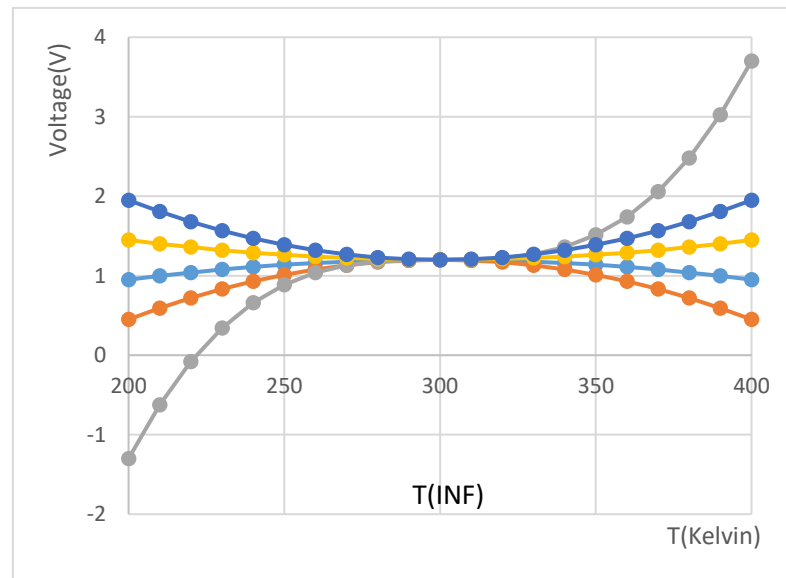
Figure 14 Several possible curvatures of reference circuit

Though the examples shown on the Figure 14 all also have the same output at T_{INF}, they could all have different outputs while still satisfying the inflection point constraint. If they have the same inflection temperature and the same output at T_{INF}, the second derivative or preferably the normalized second derivative evaluated at T_{INF}, would give an indication of relative flatness around T_{INF}. This concept will now be extended to develop a metric for comparing different bandgap circuits where the outputs at T_{INF} are not necessarily the same.
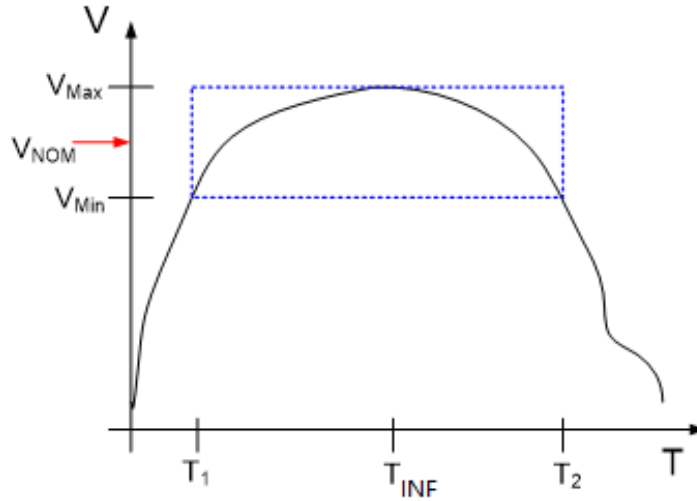
Figure 15 A example reference of bandgap reference circuit

If it can be assumed that the bandgap reference has only one peak like that depicted in Figure 15, the standard temperature coefficient expressed in equation (60), is often used as a metric for comparing performance of different references.

$$TC_{reg} = \frac{V_{Max} - V_{Min}}{(T_2 - T_1)} 10^6 \tag{60}$$

But this metric does not consider the possibility that different references will have different outputs at T_{REF}.

A better method for comparing the performance of bandgap reference circuits is to use the normalized temperature coefficient, which is been expressed like this:

$$TC_{norm} = \frac{V_{Max} - V_{Min}}{(T_2 - T_1)V_{NOM}} 10^6 \tag{61}$$

In this equation, V_{NOM} could be any output between V_{MIN} and V_{MAX}. For a good reference, that is a reference where $V_{MAX}-V_{MIN}$ is small relative V_{MAX}, it is not critical exactly what value be used for V_{NOM}. A convenient value for V_{NOM} is:

$$V_{NOM} = V_{REF}\left(T_{INF}\right) \tag{62}$$

V_{NOM} as defined in (62) will be used as the normalizing variable throughout the remainder of this thesis.

3.1.1 Relationship between Temperature Coefficients and Curvature

The reference voltage can be represented in a Taylor series expansion about the inflection point as:

$$V_{REF}(T) = V_{REF}(T_{INF}) + \sum_{k=1}^{\infty} \left. \frac{\partial^k V_{REF}}{\partial T^k} \right|_{T=T_{INF}} \frac{(T-T_{INF})^k}{k!} \tag{63}$$

If this expression is truncated after the second-order derivative term while satisfying the constraint that the first-order derivative at the inflection point is zero, the output of the reference can be expressed as in equation (64).

$$V_{REF}(T) \cong V_{REF}(T_{INF}) + \left. \frac{\partial^2 V_{REF}}{\partial T^2} \right|_{T=T_{INF}} \frac{(T-T_{INF})^2}{2} \tag{64}$$

Since this expression is symmetric around T_{INF} and since the maximum deviation in the output will occur at the extreme points on the temperature interval $[T_1 \ T_2]$ it follows that:

$$|V_{MAX}\text{-}V_{MIN}| \cong \left| V_{REF}(T_{INF}) \text{-} V_{REF}\left(T_{INF} + \frac{\Delta T}{2}\right) \right| \tag{65}$$

where $\Delta T = T_2 - T_1$.

Substituting equation (64) into equation (65), it follows that:

$$|V_{MAX}\text{-}V_{MIN}| \cong \left. \frac{\partial^2 V_{ref}}{\partial T^2} \right|_{T=T_{INF}} \frac{\left(T_{INF} + \frac{\Delta T}{2} \text{-} T_{INF}\right)^2}{2} = \left. \frac{\partial^2 V_{ref}}{\partial T^2} \right|_{T=T_{INF}} \frac{\Delta T^2}{8} \tag{66}$$

Substituting equation (66) into the equation (61) of the TC, it follows that:

$$TC_{norm} = \left. \left| \frac{\partial^2 V_{ref}}{\partial T^2} \right| \right|_{T=T_{INF}} \frac{\Delta T}{8V(T_{INF})} \tag{67}$$

According to the equation (67), TC_{norm} is dependent only upon the second-order term in the expansion, the temperature range, and the output at the output at the temperature inflection point. It can be observed that when the first-order derivative

vanishes, the normalized temperature coefficient is proportional to the curvature at the inflection temperature.

3.1.2 References with output of form a+bT+cTlnT.

For those voltage references that have an output voltage that can be expressed in the form of equation (35), the second-order derivative can be calculated and evaluated at the inflection temperature. It follows that:

$$\frac{\partial^2 V_{ref}}{\partial T}\bigg|_{T=T_{INF}} = \frac{c}{T_{INF}} \tag{68}$$

Thus, for such references, TC_{norm} can be expressed as:

$$\text{TC}_{norm} = \frac{c\Delta T}{8V(T_{INF})T_{INF}} \tag{69}$$

Since the first-order derivative of the reference voltage of these references at the temperature inflection point is equal to zero, it follows from equation (35) that:

$$\frac{\partial V_{ref}(T_{INF})}{\partial T} = b + c(1 + lnT_{INF}) = 0 \tag{70}$$

From the equation (70), the coefficient b can be expressed like this:

$$b = -c(1 + lnT_{INF}) \tag{71}$$

Substituting from equation (71) back to the equation (35) to get the reference voltage at the temperature inflection point, it follows that:

$$V(T_{INF}) = a - cT_{INF} \tag{72}$$

Substitute the equation (72) back to the equation (69), it follows that TC_{norm} can be expressed as:

$$\text{TC}_{norm} = \left|\frac{\partial^2 V_{ref}}{\partial T^2}\right|\bigg|_{T=T_{INF}} = \frac{c\Delta T}{8(a-cT_{INF})T_{INF}} \tag{73}$$

Though the equations that were obtained for several references had quite complicated expressions for the coefficient b, the expressions for a and c were much

simpler. It can be observed that the expressions for TC_{norm} can be simply expressed in terms of the parameters a and c, the temperature range, and the inflection point temperature. It must be emphasized that this functional form is only applicable to references that have an output of the form a+bT+cTlnT where the coefficients a, b and c are independent of temperature.

3.1.3 Comparison of different bandgap reference circuits

Since the references considered in Chapter 2 all had an output that can be expressed in the form a+bT+cTlnT, equation (73) can be used to express their temperature coefficient. Considering the Brokaw reference circuit as an example, and substituting from equation (36) back to equation (73), the normalized temperature coefficient can be expressed as:

$$TC_{norm} = \frac{c\Delta T}{8(a-cT_{INF})T_{INF}} = -\frac{\frac{k}{q}n\Delta T}{4(V_{G0}+2\frac{k}{q}nT_{INF})T_{INF}} \tag{74}$$

It can be observed that there are no design variables in TC_{norm} for the Brokaw reference and thus once the inflection temperature and temperature range are specified, the temperature coefficient cannot be optimized with the design variables that are available in the circuit.

The normalized temperature coefficients of all the references considered in Chapter 2 are summarized in Table 4.

Table 4 Comparison of TC of bandgap circuits

Structure Name	a	c	$TC_{normlized}$
Brokaw	V_{G0}	$-2n\dfrac{k}{q}$	$-\dfrac{\dfrac{k}{q}n\Delta T}{4(V_{G0}+2\dfrac{k}{q}nT_{INF})T_{INF}}$
Banba	$\dfrac{R_3}{R_1}V_{G0}$	$-2n\dfrac{R_3}{R_1}\dfrac{k}{q}$	$-\dfrac{\dfrac{k}{q}n\Delta T}{4(V_{G0}+2\dfrac{k}{q}nT_{INF})T_{INF}}$
Kuijk	V_{G0}	$-2n\dfrac{k}{q}$	$-\dfrac{\dfrac{k}{q}n\Delta T}{4(V_{G0}+2\dfrac{k}{q}nT_{INF})T_{INF}}$
Mietus	V_{G0}	$-2n\dfrac{k}{q}$	$-\dfrac{\dfrac{k}{q}n\Delta T}{4(V_{G0}+2\dfrac{k}{q}nT_{INF})T_{INF}}$
Mixed Bio-MOS	V_{G0}	$-2n\dfrac{k}{q}$	$-\dfrac{\dfrac{k}{q}n\Delta T}{4(V_{G0}+2\dfrac{k}{q}nT_{INF})T_{INF}}$
Alternated Banba	V_{G0}	$-2n\dfrac{k}{q}$	$-\dfrac{\dfrac{k}{q}n\Delta T}{4(V_{G0}+2\dfrac{k}{q}nT_{INF})T_{INF}}$
Modified Kuijk	V_{G0}	$-2n\dfrac{k}{q}$	$-\dfrac{\dfrac{k}{q}n\Delta T}{4(V_{G0}+2\dfrac{k}{q}nT_{INF})T_{INF}}$

Though the circuit structures for the comparative structures are different and though the expressions for the output voltages of the references are different, it can be observed that the normalized temperature coefficients for all of the comparative structures are identical. And, as for the Brokaw circuit, there are no design variables

available in any of these circuits that can be used for optimization by the designer. It can also be shown that if the output of these circuits is normalized by the output at the inflection temperature, then all circuits have the same normalized output and it is given by the expression.

$$V_{REF\_NORM}(T) \cong \frac{a - cT\left(1 - \ln\dfrac{T}{T_{INF}}\right)}{a - cT_{INF}} \tag{75}$$

Although the normalized output and the normalized temperature coefficients are not dependent upon design parameters, they are dependent upon the parameter m that appears in the c coefficient. The value of m is typically between 2 and 4 and the value of n is typically around 1. Plots of the normalized output and the normalized temperature coefficient for these circuits for m=2.3 and n=1 appear in Figure 16 and Figure 17. The corresponding plots for m=3 and n=1 appear in Figure 18 and Figure 19. Note that the normalized temperature coefficient increases by over 50% when m changes from 2.3 to 3.
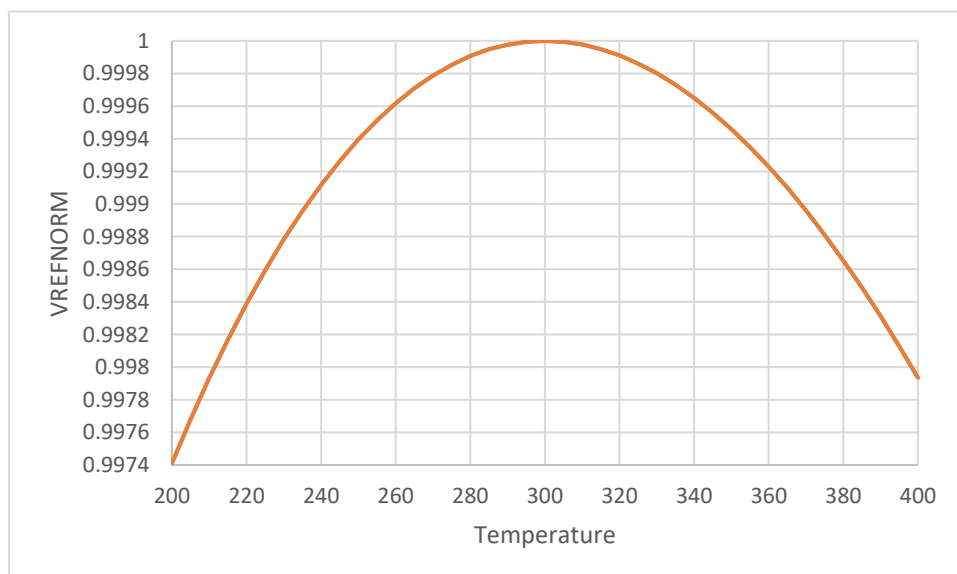

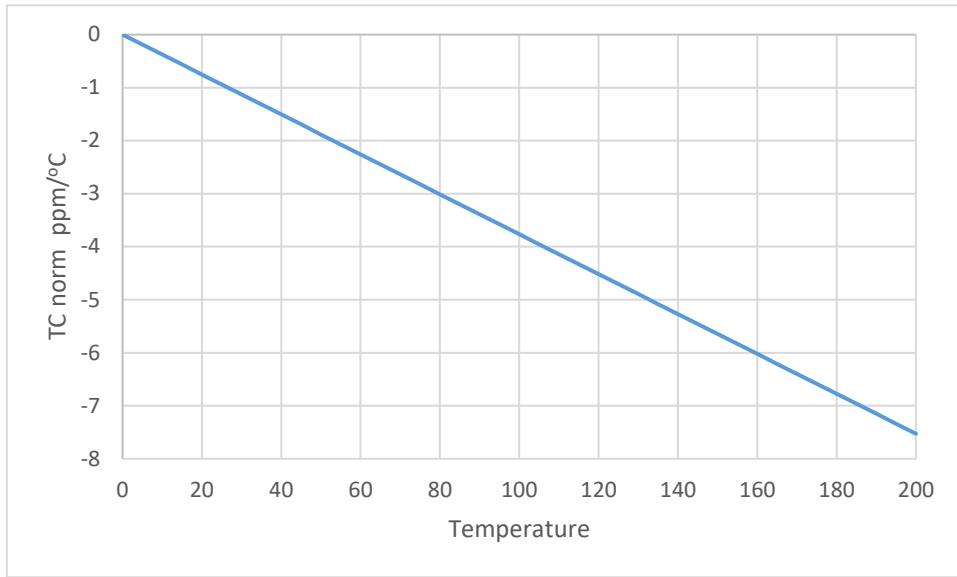Figure 16 Normalized Reference Output for m=2.3
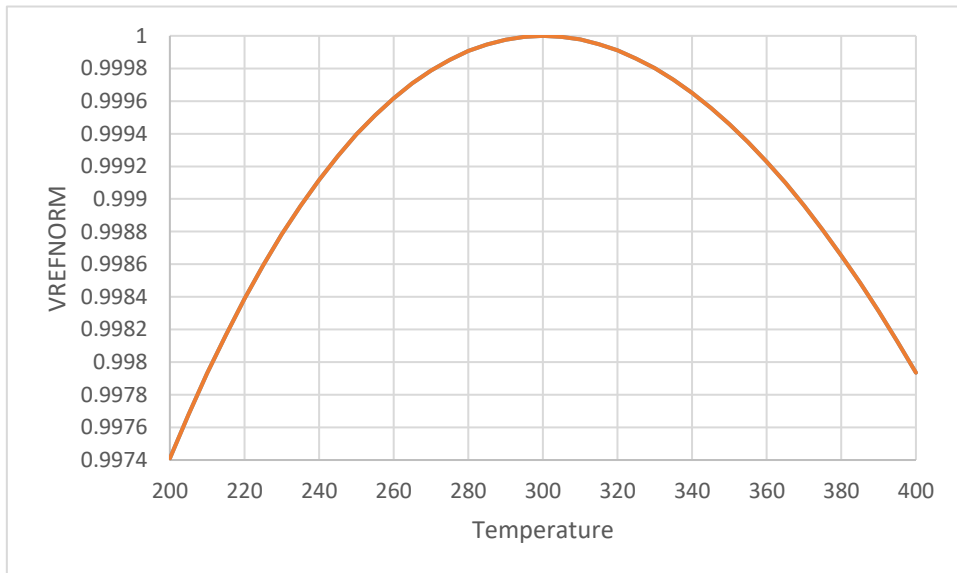
Figure 17 Normalized TC for m=2.3

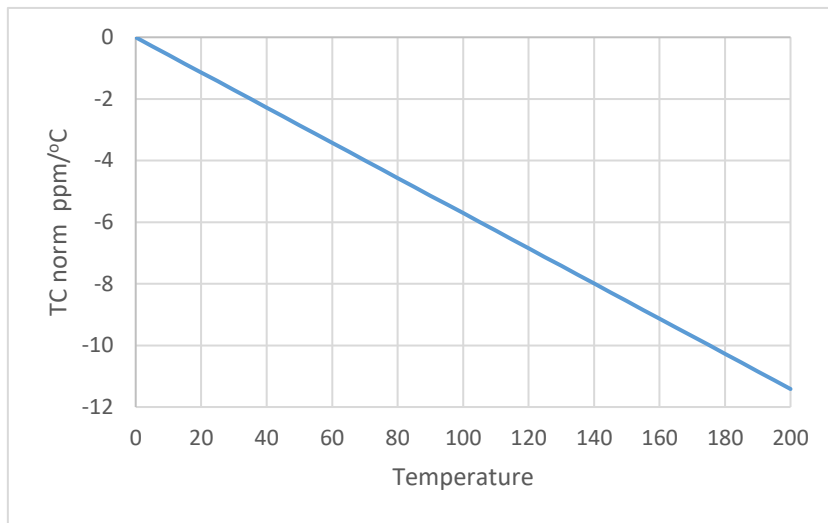Figure 18 Normalized Reference Output for m=3

Figure 19 Normalized TC for m=3

The plots in Figure 16 are particularly useful because they characterize the performance of any bandgap circuit that has an output voltage of the form a+bT+cTlnT where:

$$\frac{c}{a} = n\frac{(1-m)k}{V_{G0}q}$$

(76)

And where the PN junction is modeled by (76). More importantly, it must be emphasized that these plots not related to the complicated parameter b

3.2 Spectre Simulation Results of Reference Circuits

The analytical results obtained for the comparative bandgap circuits were based upon ideal models of the operational amplifier, the basic square-law model of the MOS transistors, temperature-independent models for the resistors, and the analytical model of the PN junction given by (76). Computer simulations that include more detailed device models will be considered for select circuits in this section. It is anticipated that these results are representative to what occurs for all circuits in the comparison group.

3.2.1 Banba reference circuit

An implementation of the Banba circuit designed in a 0.5μm CMOS process is shown in Figure 20. Although a start-up circuit is required, it is not shown in the schematic since it does not affect performance under normal operating conditions.
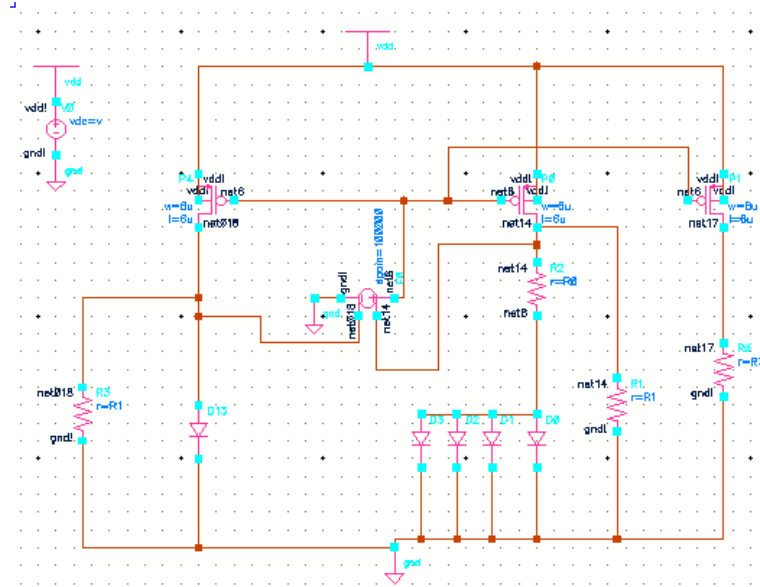
Figure 20 Banba Reference Circuit Structure

In this implementation, the MOS transistors were sized the same with a multiplier of 2. The gain of the Opamp is 80dB with no offset voltage. The ratio of the areas of D_2 and D_1 was set to 4. The remaining parameters in this design are the resistor values R_0, R_1, R_2, and R_3 with the three constraints $R_1=R_2$, $T_{INF} = 27°C$, and an output voltage level that is scaled by R_3. For convenience, to set the output voltage near 1.2V at a current level of around 30uA, the resistor R_3 was set to about 30K. The resistors R_0 and R_1 then were selected to satisfy the inflection point constraint of (71) and the equation for the polynomial coefficient b in (37).

From these relationships, it is easy to get approximate values for R_0 and R_1. Since the device models in the simulator differ a bit from the analytical model of (15), the simulator was used to twist a little to get the inflection point at $27°C$. The component values used in this design are summarized in Table 5. The temperature coefficient of the resistor was set at 0 in these simulations. Since we do not have a good device model for the diode, the model of a generic diode, given in the Appendix, was

used for the diode. In this model, m=3 and n=1.22. Spectre simulation results are given

in Figure 21.

Table 5 Simulation parameters for Banba with diode

V	5V
R_0	2K
R_1, R_2	33.63K
R_3	32.4K
$\dfrac{A_2}{A_1}$	4
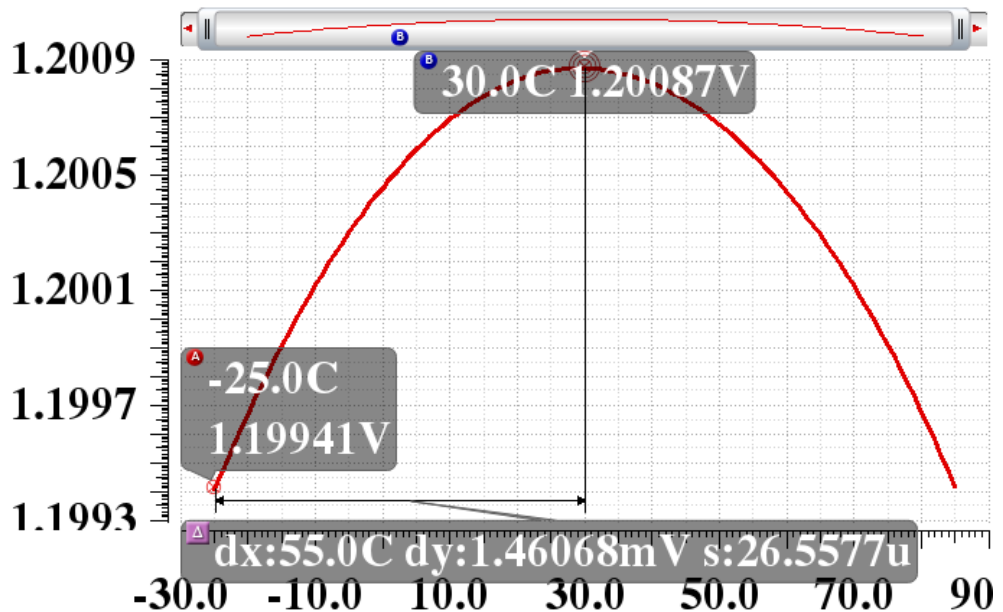
Figure 21 Banba output reference voltage

From the simulation results of Figure 21, the temperature coefficient can be

calculated:

$$\text{TC} = \frac{V_{max} - V_{min}}{(T_{max} - T_{min})V_{nomial}} 10^6 = \frac{1.46}{110 \times 1.2001} 10^3 = 11.1 ppm/°C \qquad (77)$$

The results presented in Figure 19 which are approximations for m=3, n=1, and

no temperature dependence of the resistors were 6.3ppm/°C and for m=3 and n=1.22

they become 7.6ppm/°C over the same 110°C temperature range which is about 30%

less than the Spectre simulation results.

Since a good diode is not available in the process under consideration, a diode-connected substrate PNP transistor is often used instead of the diode. The schematic with this modification, using an NPN transistor instead, is shown in the Figure 22.
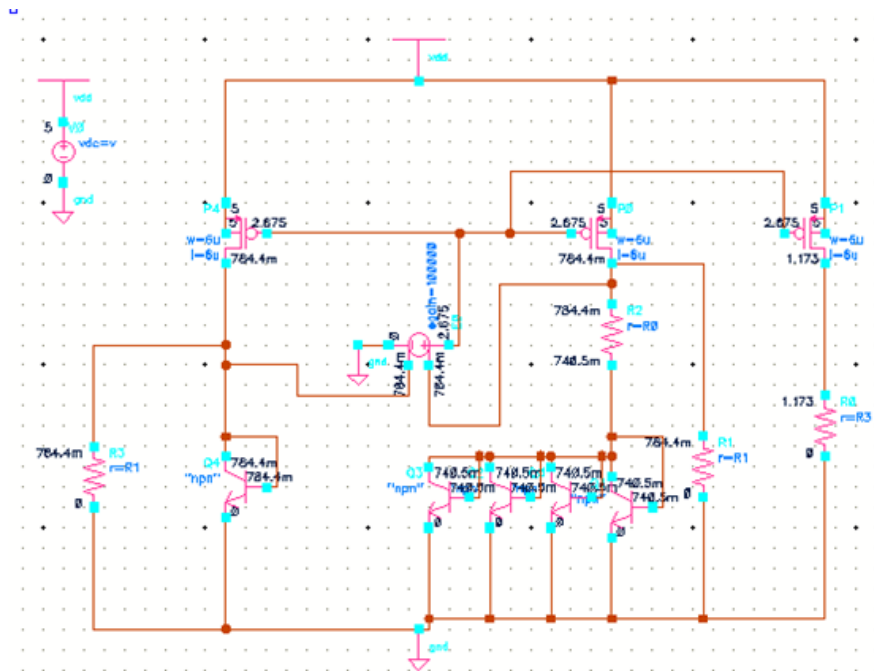
Figure 22 Banba Reference Circuit with BJT as diode

Since the characteristics of the BJT are somewhat different than the diode, minor modification of the design parameters are needed to set the inflection point at 27°C. The component values used in the design are summarized in Table 6 and the simulation results are shown in Figure 23.

Table 6 Simulation parameters for Banba with diode-BJT

V	5V
R_0	2K
R_1, R_2	29.04K

Table 6 continued

R_3	24K
$\dfrac{A_2}{A_1}$	4
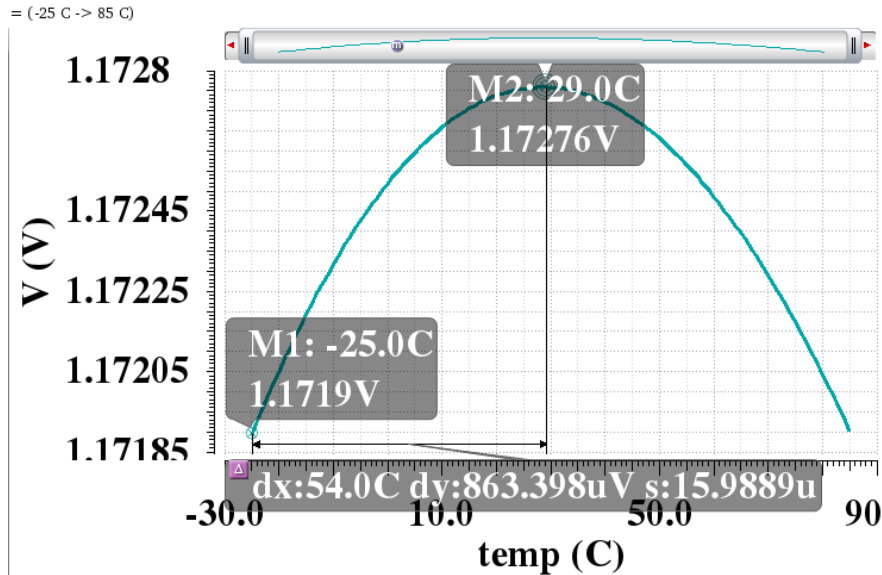
Figure 23 Output voltage of Banba with MOS as diode

From the results in Figure 23, the temperature coefficient can be calculated:

$$\text{TC} = \frac{V_{max} - V_{min}}{(T_{max} - T_{min})V_{nomial}} 10^6 = \frac{0.8634}{110 \times 1.17235} 10^3 = 6.7 ppm/°C \qquad (78)$$

The new temperature coefficient obtained with the diode-connected BJT is close to the analytical MATLAB simulation results for m=3 and n=1 of $6.3 ppm/°C$.

The performance of the bandgap reference with diode-connected BJTs show some benefits compared to what is obtained with an actual diode, as explained by Hibiber [14]. Hibiber indicated that this is due to surface effects or the generation and recombination of carriers in the depletion layer of a PN junction. Though the simulation results for the reference with the diode-connected transistors were modestly better than with a simple diode, no attempt was made to conclude the models used actually reflect the benefits identified by Hibiber.

3.2.2 Brokaw reference circuit

An implementation of the Brokaw circuit is shown in Figure 24. Although a start-up circuit is required, it is not shown in the schematic since it does not affect performance under normal operating conditions. The design strategy for setting the inflection temperature at 27°C is similar to that used for the Banba circuit.
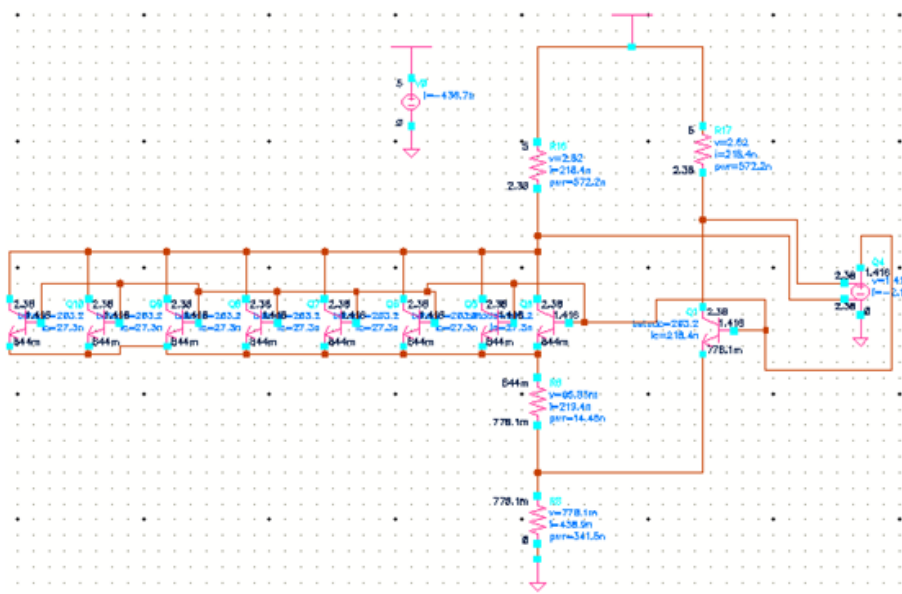
Figure 24 Brokaw Reference Circuit

In this implementation, the emitter area ratio of Q_1 to Q_2 was set at 8 instead of 4 as used for the simulation of the Banba reference circuit. Component values that set the inflection point at 27°C are shown in Table 7. The BJT model given in the Appendix was used for Q_2. Spectre simulation results for a plot of the reference voltage are shown in Figure 25.

Table 7 Simulation parameters for Brokaw with BJT

V	4V
R_1	1.773M
R_2	300K

Table 7 continued

R_3, R_4	10M
$\dfrac{A_2}{A_1}$	8
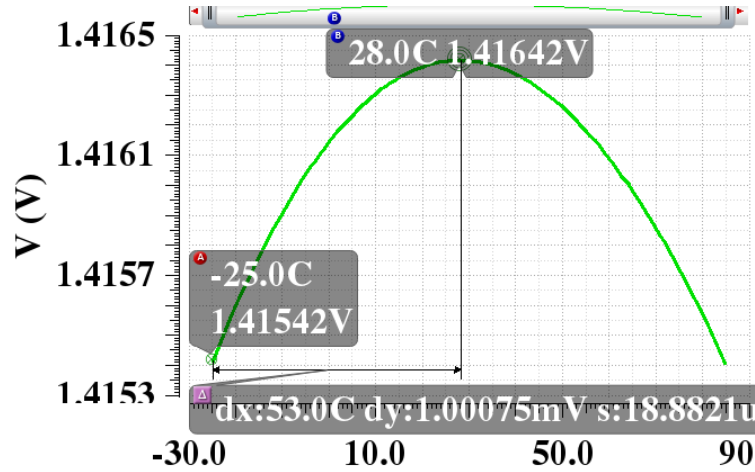
Figure 25 Output voltage of Brokaw reference circuit

From the results shown in Figure 25, the temperature coefficient can be calculated:

$$\text{TC} = \frac{V_{max} - V_{min}}{(T_{max} - T_{min})V_{nomial}} 10^6 = \frac{1}{110 \times 1.416} 10^3 = 6.42 ppm/°C \qquad (79)$$

This result is close to the analytical results of $6.3 ppm/°C$ shown in Figure 19 obtained for m=3 and n=1.

3.2.3 Kuijk reference circuit

An implementation of the Kuijk reference circuit is shown in Figure 26. Although a start-up circuit is required, it is not shown in the schematic since it does not affect performance under normal operating conditions. Spectre result of an implementation of this circuit will also be compared with the analytical results presented previously.

Figure 26 Kuijk Reference Circuit Structure

Initially the model given in the Appendix will be used to model the diodes. Design parameters that place the inflection point at 27°C are given in Table 8. A plot of the reference voltage versus temperature obtained with the Spectre simulation is shown in Figure 27.

Table 8 Simulation parameters for Kuijk with diode

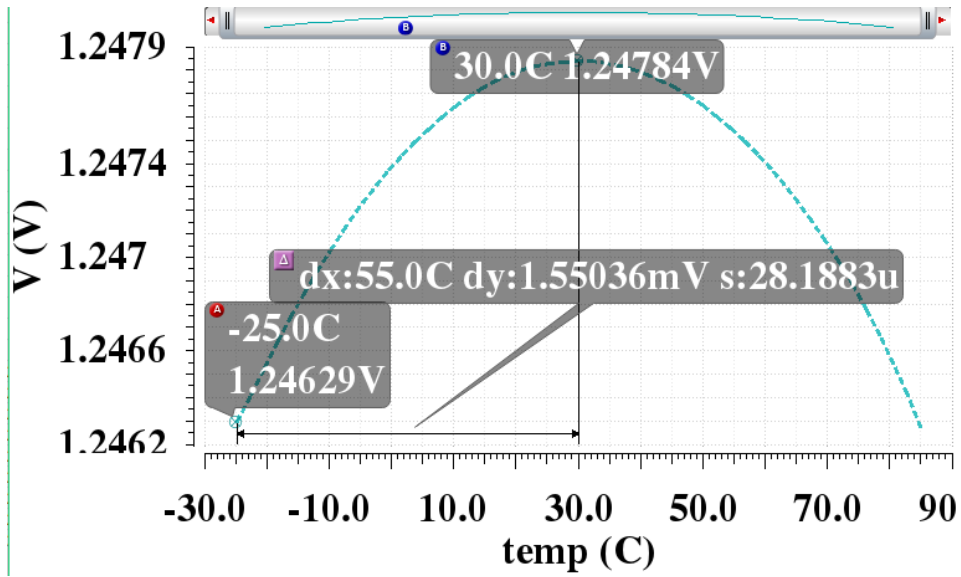| V	5V
R_0	3.609k
R_1, R_2	62k
$\dfrac{A_2}{A_1}$	4

Figure 27 Output voltage of Kuijk reference circuit

From this plot, the temperature coefficient can be calculated:

$$\text{TC} = \frac{V_{max} - V_{min}}{(T_{max} - T_{min})V_{nomial}} 10^6 = \frac{1.55}{110 \times 1.247} 10^3 = 11.3 ppm/°C \qquad (80)$$

These results are comparable to what was obtained for the Banba circuit using

the same model for the diodes and they differ modestly from the 7.6ppm/°C that was

obtained for the same 110°C temperature range obtained from the analytical derivation

with m=3 and n=1.22.

As with the Banba circuit, Spectre simulations were also made using diode-

connected transistors instead of the simple diodes. In the Spectre simulation, the diode-

connected transistor Q₁ was modeled with the NPN transistor model given in the

Appendix. The circuit schematic corresponding to the diode-connected transistor

configuration is shown explicitly in the Figure 28. Design parameters that place the

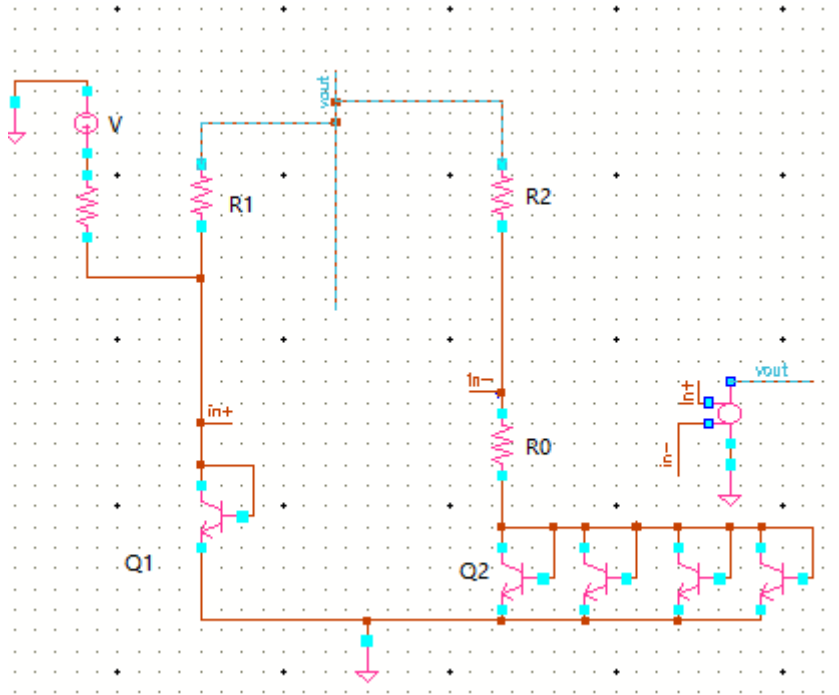inflection point at 27°C are given in Table 9.

Figure 28 Kuijk reference circuit with diode-BJT

A plot of reference voltage versus temperature obtained from the Spectre simulation is shown in Figure 29.

Table 9 Simulation parameters for Kuijk with diode-BJT

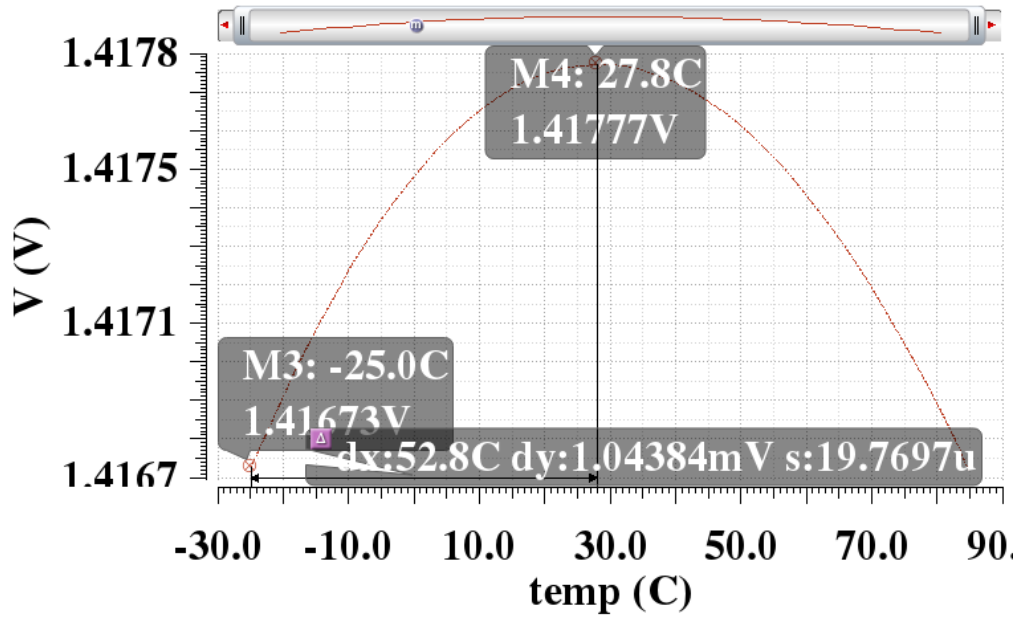|	
V	5V
R_0	4145
R_1, R_2	62k
$\dfrac{A_2}{A_1}$	4

Figure 29 Output voltage of Kuijk with diode-MOS

From the simulation results shown in Figure 29, the temperature coefficient

can be calculated:

$$\text{TC} = \frac{V_{max} - V_{min}}{(T_{max} - T_{min})V_{nomial}} 10^6 = \frac{1.04384}{110 \times 1.4173} 10^3 = 6.7 ppm/°C \qquad (81)$$

These results are also comparable to what was obtained with the Banba

reference circuit using diode-connected transistors and close to the $6.3\ ppm/°C$

obtained with the analytical formulation with m=3 and n=1.

3.3 Performance Assessment of Selected Traditional Bandgap Reference Circuits

From both the analytical formulations and simulation results presented in this

chapter, several observations can be made about the selected group of traditional

bandgap reference circuits. Firstly, the second-order derivative of the reference voltage

with respect to temperature is determined by the parameters a and c for all references

in this select comparison group. Secondly, the normalized temperature coefficient is

only related to the parameters a and c and is obtained directly from the second-order

temperature derivative. Thirdly, the temperature coefficient is independent of the design

variables for all circuits in this select group. Fourth, and most importantly, if the technology is same, the temperature coefficient is the same for all structures in this select group. Finally, the small difference between analytical and Spectre simulations is due to small differences in the models.

Based upon the discussions that appeared in the papers where the different structures were introduced and based upon the lack of comparisons by the original authors, one would be tempted to conclude that there would be considerable differences in performance of these structures. One would also be tempted to conclude that the performance of each of the structures could be optimized through judicious choice of the design variables. However, it has been shown that if the temperature range, temperature inflection point, and the method to calculate the temperature coefficients are the same, the truth is that all of these structures exhibit about the same temperature-related performance. The structures may, however, differ in voltage reference range, supply voltage range, and power dissipation.

CHAPTER IV NON-BANDGAP REFERENCE CIRCUIT

The reference circuits considered in Chapter 2 are termed "bandgap" reference. They all have the unique property that the output voltage is approximately proportional to the bandgap voltage of silicon which is generally considered to be a physical constant. Though the structures were considerably different, it was shown that all of the selected popular bandgap circuits considered in Chapter 2 exhibited the same normalized temperature coefficient. The fundamental properties of these bandgap circuits were all derived by extracting, in some way, the bandgap voltage of silicon from one or more PN junctions with clever circuit structures.

As CMOS technology is becoming increasingly dominant in industry, it may be worthwhile to explore if the dominant device in a CMOS process, the MOSFET, can replace the traditional PN junction in the design of voltage references while also providing better performance. There are two well-defined mode of operation of a MOSFET, strong inversion and weak inversion and in both to these modes there are three well-defined regions of operation for the MOSFET; cutoff, triode and saturation region. The use of the MOSFET in the design of a voltage reference circuit in both Weak Inversion and Strong Inversion will be considered.

4.1 Weak Inversion Operation of MOSFET

The term "sub-threshold region" region is used interchangeably with the term "weak inversion". And either of these regions are sometimes referred to operating in the cutoff region. The cutoff region is often characterized by operation when $V_{gs} < V_{th}$. In the vicinity of $V_{gs}=V_{th}$, a region that is sometimes referred to as "moderate inversion",

the device model is quite complicated. In this work, emphasis on the weak-inversion

mode of operation will be restricted to operating conditions where $V_{gs}<V_{th}-4V_T$.

Under this assumption, the weak inversion model of the MOSFET can be expressed as;

$$\begin{cases} I_D = \frac{2\mu C_{ox}n^2V_T^2}{e^2}\frac{W}{L}e^{\frac{V_{gs}-V_{th}}{nV_T}}\left(1-e^{-\frac{V_{ds}}{nV_T}}\right) & V_{ds} < 4V_T \\ \\ I_D = \frac{2\mu C_{ox}n^2V_T^2}{e^2}\frac{W}{L}e^{\frac{V_{gs}-V_{th}}{nV_T}} & V_{ds} \geq 4V_T \end{cases} \tag{82}$$

When the V_{ds} is larger than four times the thermal voltage, the drain current

can be expressed as:

$$I_D \cong \left[\frac{2\mu C_{OX}n^2V_T^2}{e^2}\frac{W}{L}e^{-\frac{V_{th}}{nV_T}}\right]\bullet e^{\frac{V_{GS}}{nV_T}} \tag{83}$$

It can be observed from (83) that operation is much like that of the diode or

bipolar transistor in that there is an exponential relationship between the drain current

and the corresponding gate-source voltage. There is also considerable similarity

between the coefficient term $\left[\frac{2\mu C_{OX}n^2V_T^2}{e^2}\frac{W}{L}e^{-\frac{V_{th}}{nV_T}}\right]$ and the corresponding term in the

model of the diode or the BJT though the bandgap voltage is absent in this coefficient

for the MOSFET.

4.2 Weak inversion based Banba reference circuit

The idea of making use of the MOS transistor in a voltage reference is not new.

In the late 1970's Tsividis and Vittoz reported incorporating MOS transistors operating

in the weak inversion region [16][17] in voltage reference circuits. However, in these

works, the MOS transistor was not a direct replacement of the diode in a diode-based

reference circuit. More recently Ueno [18] introduced a CMOS voltage reference

circuit with devices operating in the subthreshold region where emphasis was placed

on operating at very low current levels. Geiger, Allen, and Strader [11] mentioned a voltage reference circuit in which diodes were directly replaced with MOS transistors operating on the weak inversion region but did not provide a detailed assessment of the performance of the circuit.

Consider the circuit structure shown in Figure 30 Banba reference circuit with MOSFET in which the two MOS transistors, M_1 and M_2, are assumed to be operating in weak inversion. The structure is the same as the Banba reference circuit [10] except the diodes in the Banba circuit have been replaced with MOS transistors operating in weak inversion saturation.
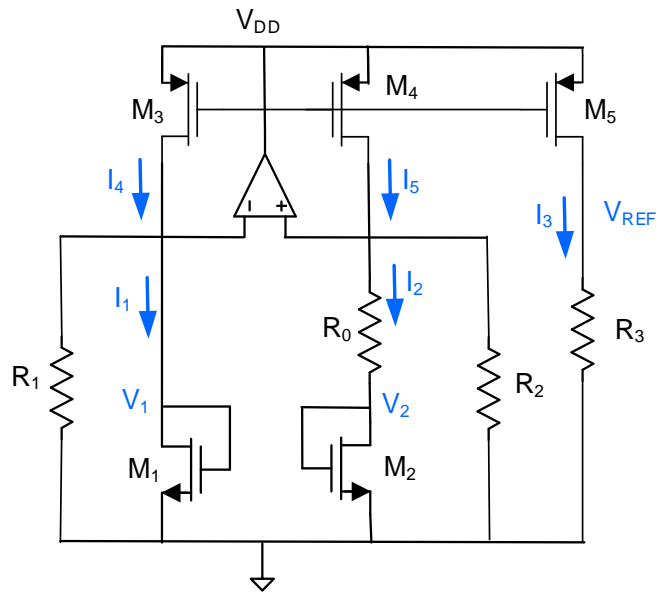
Figure 30 Banba reference circuit with MOSFET

To keep the MOS transistors M_1 and M_2 operating in weak inversion saturation, the voltages V_1 and V_2 are constrained by the inequalities and V_T is the thermal voltage:

$$\begin{cases} 4V_T < V_1 < V_{th} - 4V_T \\ 4V_T < V_2 < V_{th} - 4V_T \end{cases} \tag{84}$$

One of the benefits of operating in weak-inversion is the low power dissipation potential inherent when currents are very small. However, if extremely small currents

flow through resistors, the resistor values would be needed to be very large to maintain reasonable voltage levels. The key currents in the circuit of Figure 30 will be very small resulting in the requirement for very large resistors. As such, this circuit may be applicable only in processes that have a very high sheet resistance option available. In this work, only Spice simulations will be considered and the size of resistors will not be addressed further.

If it is assumed that the devices M_3, M_4, and M_5 are sized the same, a standard circuit analysis can be used to obtain the set of 8 independent equations given in (85) in the 8 unknowns $\{V_{REF}, V_1, V_2, I_1, I_2, I_3, I_4, I_5\}$. The analysis is similar to that used to derive the equation set given in (37).

$$\left.\begin{aligned}
V_1 &= V_2 + I_2 R_0 \\
I_4 &= I_1 + \frac{V_1}{R_1} \\
I_5 &= I_2 + \frac{V_1}{R_2} \\
I_1 &= \left[\frac{2\mu C_{OX} n^2 V_T^2}{e^2}\left(\frac{W}{L}\right)_1 e^{-\frac{V_{th}}{nV_T}}\right] \bullet e^{\frac{V_1}{nV_T}} \\
I_2 &= \left[\frac{2\mu C_{OX} n^2 V_T^2}{e^2}\left(\frac{W}{L}\right)_2 e^{-\frac{V_{th}}{nV_T}}\right] \bullet e^{\frac{V_2}{nV_T}} \\
V_{REF} &= R_3 I_3 \\
I_3 &= I_4 \\
I_3 &= I_5
\end{aligned}\right\} \tag{85}$$

where the model parameters of M_1 and M_2 are assumed to be identical.

The mobility and threshold voltage are both temperature dependent and can be expressed as

$$\mu = K_\mu T^{-1.5} \tag{86}$$

$$V_{th} = V_{th0} + \alpha_{vth}T \tag{87}$$

where K_μ, V_{th0} and α_{vth} are model parameters. The parameter V_{th0} is the threshold voltage projected to zero kelvin.

Substituting (86) and (87) into (85) and solving, it follows from a straightforward but tedious analysis that:

$$V_{ref} = R_3 V_{th0} + R_3 T\left(\alpha_{vth} + \frac{1}{R_0}n\frac{k}{q}\ln\left(\frac{(\frac{W}{L})_2}{(\frac{W}{L})_1}\right) + n\frac{k}{q}\ln\left(\frac{n}{R_0 K_\mu C_{ox}\frac{k}{q}(\frac{W}{L})_1}\ln\left(\frac{(\frac{W}{L})_2}{(\frac{W}{L})_1}\right)\right)\right) + R_3 0.5n\frac{k}{q}T\ln T \tag{88}$$

It can be observed from equation (88), that the reference voltage of the MOS-based reference working in the subthreshold region can also be formatted like equation (35), and the parameter can be expressed like this:

$$\begin{cases} a = R_3 V_{th0} \\ b = R_3\left(\alpha_{vth} + \frac{1}{R_0}n\frac{k}{q}\ln\left(\frac{(\frac{W}{L})_2}{(\frac{W}{L})_1}\right) + n\frac{k}{q}\ln\left(\frac{n}{R_0 K_\mu C_{ox}\frac{k}{q}(\frac{W}{L})_1}\ln\left(\frac{(\frac{W}{L})_2}{(\frac{W}{L})_1}\right)\right)\right) \\ c = R_3 0.5n\frac{k}{q} \end{cases} \tag{89}$$

Correspondingly, the temperature coefficient can be calculated from the equation (73) and expressed as:

$$TC_{norm} = \frac{c\Delta T}{8(a - cT_{INF})T_{INF}} = \frac{0.5kn}{q(V_{th0} - 0.5n\frac{k}{q}T_{INF})T_{INF}} \tag{90}$$

Details about an implementation of the sub-threshold Banba circuit are given in Table 10. The corresponding simulation results based upon the analytical expression of (88) are shown in Figure 31. It can be observed that the voltage variation is 40μV over 100℃ and therefore the temperature coefficient over 100℃ is only 0.3ppm/℃ .

From these simulation results, two significant differences between the sub-threshold MOS version of the Banba circuit and the corresponding PN-junction based

version given in Figure 8 can be observed. First, the output of the sub-threshold MOS

structure is concave upward instead of concave downward. And second, the magnitude

of the temperature coefficient is much smaller than that of the PN-junction based

structure. Comparing over the same $100^{\circ}C$ temperature range, the temperature

coefficient is about a factor of 6 lower than the 2 ppm/$^{\circ}C$ obtained for the PN-junction

based structure

Table 10 Parameters to build reference circuit of sub-thres MOS

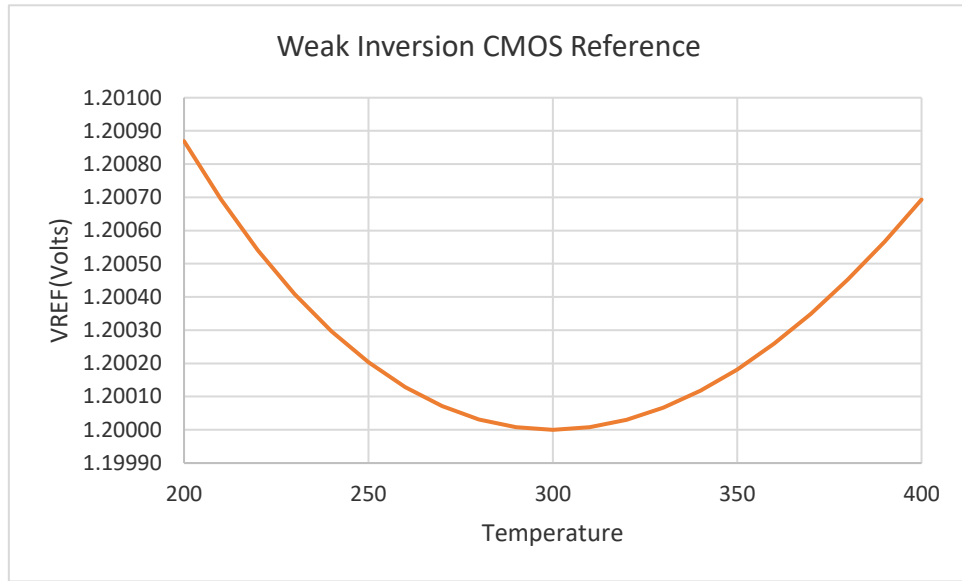|	
I_S	1.24E-08
$\mu_0 C_{ox}$	6.61E+00
V_{th0}	1.1
α_{vth}	-0.0015
n	1
T_{INF}	300
$\dfrac{J_1}{J_2}$	1.2
a	0.802
b	$6.0744E-06$

Figure 31 Weak Inversion Output Voltage of the Banba Structure

4.3 Strong Inversion Operation of MOSFET

When the $V_{gs} > V_{th}+4V_T$, the transistor operates in strong inversion with a nearly square-law relationship between drain-current and V_{gs} when operating in the saturation region (91):

$$I = \frac{\mu C_{ox} W}{2L}(V_{gs} - V_{th})^2 \tag{91}$$

The Banba circuit can also be used as a voltage reference when the MOSFETs are operating in strong inversion. Though not presented here, it can be readily shown that the output of a reference with strong-inversion transistors is concave upward with a rather large temperature coefficient relative to that achieved with weak-inversion MOSFETs or bipolar devices.

4.4 Simulation results

The results presented in the previous section were based upon analytical models for the MOS transistors operating in weak inversion. These analytical models do not include parasitic devices, such as the reverse-biased PN junctions that are inherent in a bulk CMOS process. Details about the exact models used in commercial circuit

simulators such as Spectre are difficult to obtain as well. In this section Spectre simulation results will be obtained and compared with the analytical results of the previous section.

Initial Spectre simulations for the weak-inversion Banba circuit designed in an ON 0.6µm CMOS process differed considerably from the analytical results and will not be discussed here. But two implementations of the Banba circuit designed in the ON 0.6µm CMOS process will be considered. One is for devices operating in deep weak inversion and the other is for devices operating in moderate inversion.

4.4.1 Weak inversion based reference circuit

A schematic from CADENCE for the Banba reference circuit using MOSFETs operating in weak inversion is shown in Figure 32.
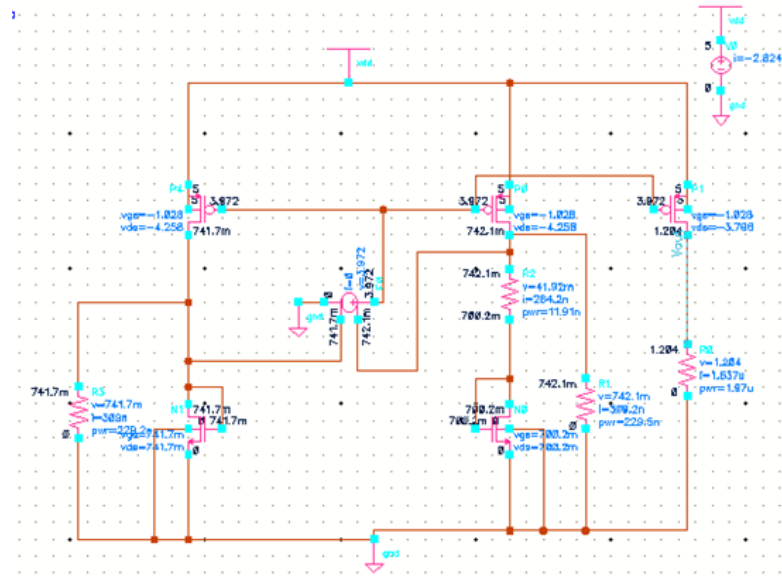

Figure 32 MOSFET working in sub-thres with Banba reference structure

As mentioned above, the analytical models did not include the diffusion parasitic. Simulation results showing a plot of the bulk-drain I_{BD} are shown in Figure 31.
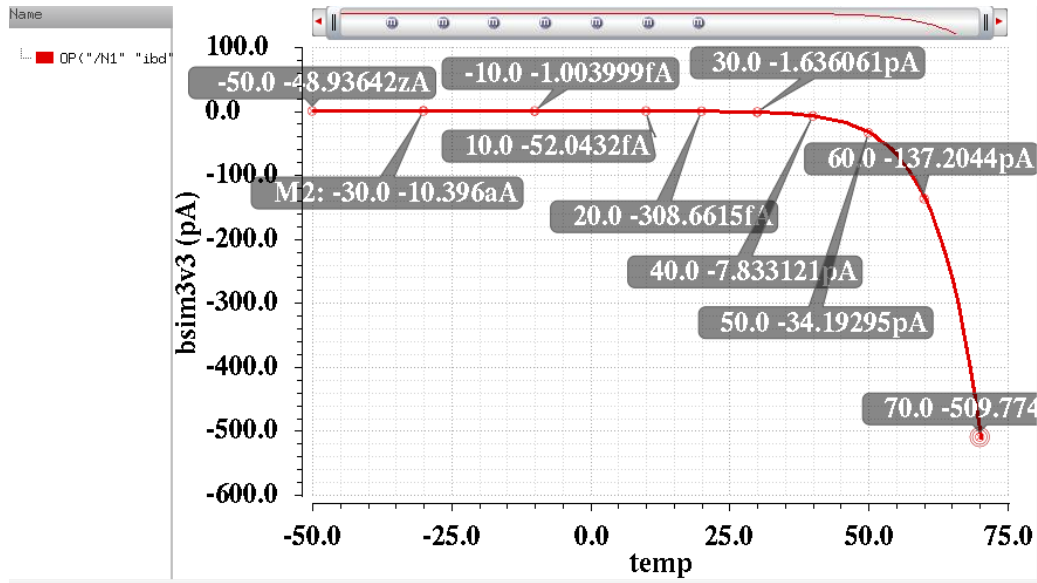
Figure 33 Bulk-Drain current versus temperature

From these simulation results, it can be observed that the bulk-drain current increases dramatically after $50°C$. In an attempt to minimize the effects of this highly temperature-dependent leakage current, the bandgap circuit was designed for an inflection temperature of 0ºC. This represents a modest downward shift in the inflection temperature from what was considered in the analytical results section. Details about the design are summarized in Table 11.

Table 11 Simulation parameters for Banba with MOS in sub-thres

V	5V
R_0	147.5k
R_1, R_2	2.4M
R_3	735.5k
$\dfrac{W_2}{W_1}$	8
$M_{3,4}$	$9\mu * 1.5\mu$

Table 11 continued

M_5	$9\mu * 0.9\mu$

Before presenting simulation results for the reference, subthreshold operation of the MOSFETs will be verified. The relationship between the gate-source voltages of M_1 and M_2 and the threshold voltages for different temperatures are shown in Table 12. Comparing with the conditions for weak inversion operation given in equation (84), it can be observed that M_1 and M_2 are operating in weak inversion.

Table 12 Voltage limitation and verification

Temperature (°C)	Threshold Voltage (V)	Thermal Voltage (mV)	V1 & V2 reasonable range (V)	V1 Actual Value (V)	V2 Actual Value (V)
-40	0.834	20.1	(0.084, 0.754)	0.741	0.7
5	0.797	24.0	(0.096, 0.701)	0.686	0.637
50	0.759	27.8	(0.111, 0.648)	0.631	0.574

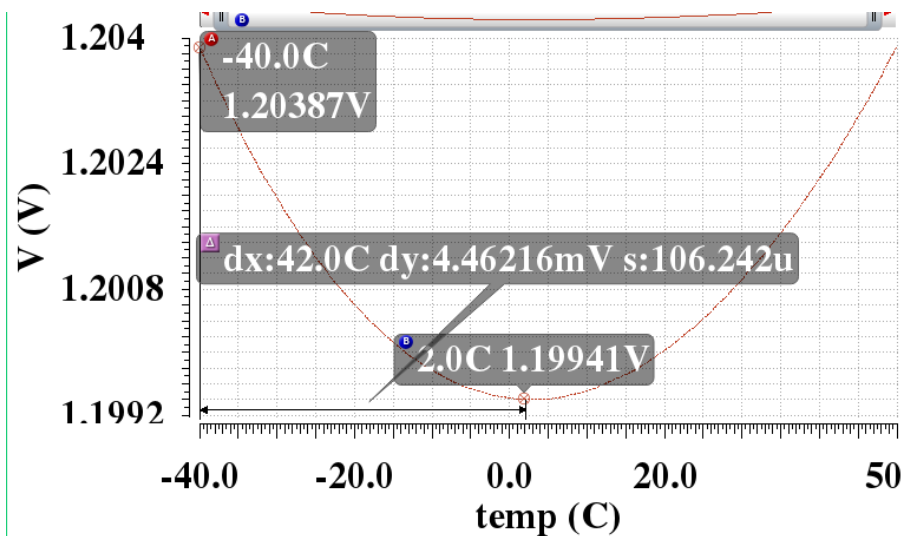Simulation results for the sub-threshold reference are shown in Figure 34.

Figure 34 Output Voltage of the Banba Reference Circuit

From the simulation results, the temperature coefficient can be calculated. For this design, the temperature coefficient is shown in equation (92):

$$TC = \frac{V_{max}-V_{min}}{(T_{max}-T_{min})V_{nomial}}10^6 = \frac{4.46}{90\times1.201}10^3 = 41.3ppm/°C \qquad (92)$$

Though the curvature characteristics are concave upward as analytically predicted and as shown in Figure 34 , the magnitude of the temperature coefficient is much larger than what was predicted analytically.

The reasons for the difference between the Spectre simulation results and the analytical results are attributable of model error both of the weak-inversion operation of the MOSFET and the leakage current in the parasitic reverse-biased PN juntions.

4.4.2 Moderated region based reference circuit

Even though the analytical formulation for the MOSFET working in strong inversion is not as good as that for the MOSFET working in the subthreshold region, there is little insight into how the reference will perform if the devices are operating in between these two regions. This intermediate region is termed the moderate inversion region. A CADENCE schematic of the Banba circuit designed to operate in moderate inversion is shown in Figure 35.
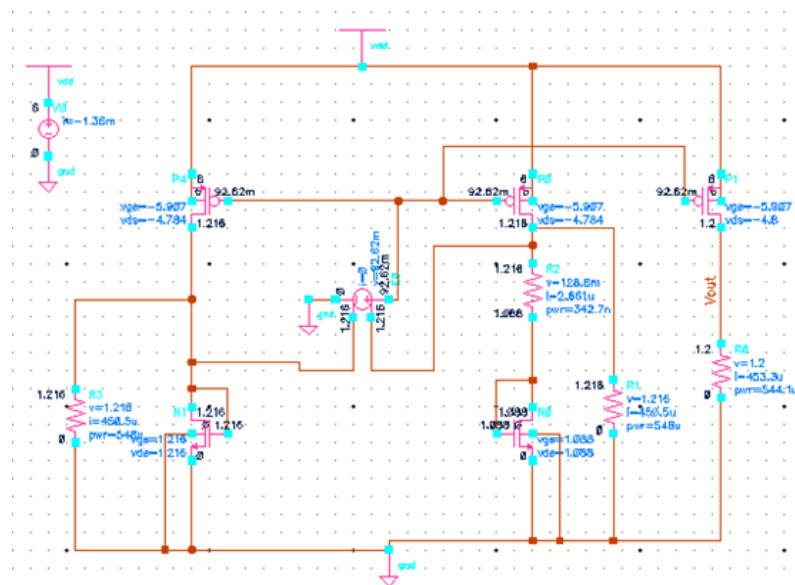

Figure 35 MOSFET working in moderate region with Banba reference circuit

Moderate inversion operation is characterized by the inequality of equation (93) shown below:

$$V_{th} - 4V_T < V_{gs} < V_{th} + 4V_T \tag{93}$$

The circuit parameters for a circuit designed to operate in moderate inversion appear in Table 13.

Table 13 Simulation parameters for Banba with MOS in moderate

V	6V
R_0	48.4k
R_1, R_2	2.7k
R_3	2.648k
$\dfrac{W_2}{W_1}$	8
$M_{3,4,5}$	$2*6\mu*6\mu$

Simulation results for V_{gs} for several different temperatures are shown in Table 14. It can be observed that M_1 and M_2 are operating in moderate inversion as desired.

Spectre simulation results for moderate inversion circuit shown in Figure 36.

Table 14 Limitation of the Vgs when MOSFET working in moderate region

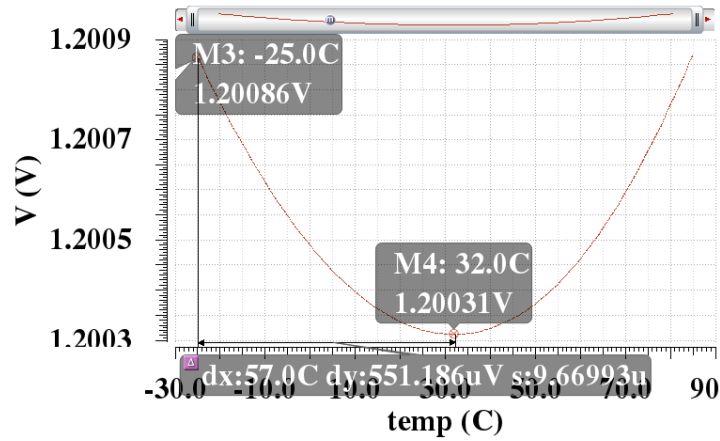| Temperature(℃)	Threshold Voltage(V)	Thermal Voltage(mV)	V1 & V2 reasonable range(V)	V1 Actual Value(V)	V2 Actual Value(V)
-25	0.821	21.38	(0.735, 0.907)	0.875	0.801
30	0.775	26.12	(0.671, 0.879)	0.84	0.751
85	0.729	30.86	(0.606, 0.852)	0.805	0.701

Figure 36 Output Voltage that MOS working in the moderate region

From the simulation results, it can be observed that the temperature coefficient of this circuit over a 110°C temperature range, as shown in equation (94), is 4.2 ppm/°C.:

$$\text{TC} = \frac{V_{max} - V_{min}}{(T_{max} - T_{min})V_{nomial}} 10^6 = \frac{0.551}{110 \times 1.2006} 10^3 = 4.2 ppm/°C \qquad (94)$$

These simulation results much better than what was obtained for the design in which MOSFET was operating in deep subthreshold region and even better than that achieved for the original bandgap reference circuit using diode-connected transistors.

Spectre simulations of other designs with the key devices operating in the moderate inversion region obtained by cleverly twisting the resistor values will likely show even better performance. Whether the good simulated performance in moderate inversion will actually be achieved if the circuit is fabricated is not known. Unfortunately, good analytical models in moderate inversion are not available and if they were, they would be mathematically complicated. And, good temperature-dependent models in moderate inversion would be even more difficult to obtain. But the improved performance of Spectre simulations should at least justify fabricating test structures to see if good performance in the moderate inversion is actually achievable, and if so, if such a design is practical.

CHAPTER V COMPARISION OF BANDGAP AND NON-BANDGAP

From the theoretical analysis of chapter 2 and 4, it is not hard to get a comparison of performance of bandgap and non-bandgap reference circuit. The normalized temperature coefficient for the bandgap reference circuit is in equation (95):

$$TC_{norm} \cong -\frac{nk\Delta T}{4qT_{INF}(V_{G0}+\frac{2nk}{q}T_{INF})} \tag{95}$$

For the non-bandgap reference circuit, the normalized temperature coefficient is in equation (96):

$$TC_{norm} \cong \frac{nk\Delta T}{16q(V_{th0}-0.5\frac{nk}{q}T_{INF})T_{INF}} \tag{96}$$

It is still not obvious to get a comparison to tell which temperature coefficient is smaller under same condition from these two equations, and for convenient and efficient comparison, Figure 37 shows the normalized result of output voltage. The figure shows obviously that the curvature of non-bandgap reference circuit has better performance than the bandgap reference circuit. Referring to the equation (61) to calculate the temperature coefficient, it is obvious that under the same temperature range and V_{ref}, the smaller difference of voltage would get smaller temperature coefficient. And the smaller temperature coefficient is what engineers want.
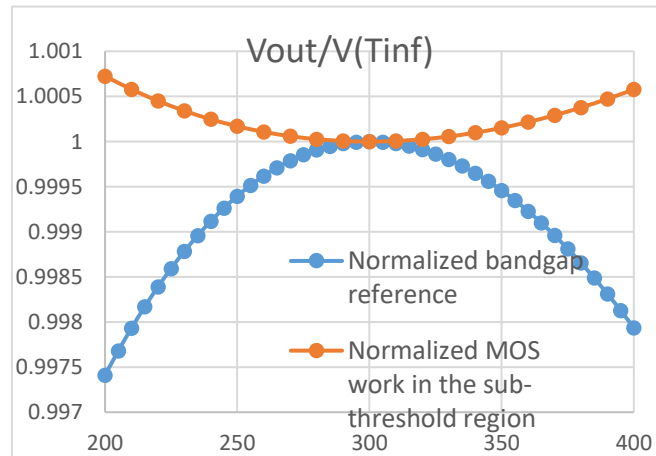

Figure 37 Normalized output voltage of bandgap and non-bandgap circuit

CHAPTER VI CONCLUSION AND IMPROVEMENT

It has been shown that closed-form analytical expressions for the output voltage of several of the most popular bandgap references can be readily obtained. And, the functional form of the output voltages as a function of temperature for all reference in the comparison group were the same. It was also shown that all references in the comparison group have identical normalized temperature coefficients. Furthermore, it was shown that though there are several degrees of freedom available to the circuit designer for each of the references in the comparison group, these degrees of freedom can not be used to improve the temperature coefficient.

Analytical results for a bandgap circuit using MOSFETs working in the sub-threshold region rather than PN junctions showed better results than what is achievable with the original bandgap reference circuits. Spectre simulation results, however, were not in close agreement with the analytical formulation. Spectre simulation results for a reference circuit designed with the MOSFETs operating in the moderate inversion region showed the best performance among all of the Spectre simulation results for all reference circuits in a 0.6μm process but this good performance was not analytically verified and it is not known whether these simulation results are predictive of what can be expected after fabrication.

APPENDIX KEY MODEL PARAMETERS

Key model parameters of typical Diode

$J_{SO}A$=1.8e-12, m=3, n=1.2

Key model parameters of typical NPN BJT

$J_{SO}A$ =3.3E-16, β=200 m=3 n=1.2

REFERENCE

[1] https://en.wikipedia.org/wiki/Bandgap_voltage_reference

[2] Hamer, Walter J. "Standard Cells: Their Construction, Maintenance, and Characteristics", National Bureau of Standards Monograph #84. US National Bureau of Standards, Jan. 15, 1965

[3] "Electric units and standards". Circular of the National Bureau of Standards. Washington, D.C.: USA Government Printing Office. 1916 (58): 39. 25 September 1916

[4] R. Widlar, "Designing Positive Voltage Regulators", EEE, Vol. 17, pp. 90-97, June 1969.

[5] R. Widlar, "New Developments in IC Voltage Regularor", IEEE Journal of Solid State Circuits, Vol. 6, pp. 2-7, Feb. 1971.

[6] P. Brokaw, "A Simple Three-Terminal IC Bandgap Reference", IEEE Journal of Solid State Circuits, Vol. 9, pp. 388-393, Dec. 1974

[7] Phillip E. Allen and Douglas R. Holberg, "CMOS Analog Circuit Design", Oxford University Press, 2002.

[8] K. Kuijk, "A Precision Reference Voltage Source", IEEE Journal of Solid State Circuits, Vol. 8, pp. 222-226, June 1973.

[9] S. M. Sze and Kwok K. Ng, "Physics of Semiconductor Devices", Wiley, 2006

[10] H. Banba, H. Shiga, A. Umezawa, T. Miyaba, T. Tanzawa, A. Atsumi, and K. Sakkui, "A CMOS Bandgap Reference Circuit with Sub-1-V Operation", IEEE Journal of Solid-State Circuits, Vol. 34, pp. 670-674, May 1999.

[11] Geiger, Allen and Strader, "VLSI Design Techniques for Analog and Digital Circuits", McGraw Hill, 1990

[12] J. J. Ebers and J. L. Moll, "Larger Signal Behavior of the Junction Transistor," Proc. IRE, Vol. 42. pp. 1761-1772, Dec, 1954

[13] D. Mietus, "Reference Voltage Circuit Having a Substantially Zero Temperature Coefficient", US Patent No. 5666046, Sept. 1997.

[14] D. Hibiber, "A /New Semiconductor Voltage Standard", IEEE Journal of Solid State Circuits, Feb. 1964

[15] Jong Mi Lee, Youngwoo Ji, Seungnam Choi, Young-Chul Cho, Seong-Jin Jang, Joo Sun Choi, Byungsub Kim, Hong-June Park and Jae-Yoon Sim, "A 29Nw Bandgap Reference Circuit", International Solid-State Circuits Conference, Feb 2015

[16] Y. P. Tsividis and R. W. Ulmer, "A CMOS Voltage Reference", IEEE Journal of Solid State Circuits, Vol. SC-13 No.6, pp. 774-778, Dec. 1978

[17] Eric A. Vittoz and Olivier Neyroud, "A Low-Voltage CMOS Bandgap Reference", IEEE Journal of Solid State Circuits, Vol. SC-14, pp. 573-577, Jun. 1979

[18] K. Ueno, T. Hirose, T. Asai and Y. Amemiya, "A 300nW, 15ppm/C, 20 ppm/V CMOS Voltage Reference Circuit Consisting of Subthreshold MOSFETs", IEEE Journal of Solid State Circuits, Vol. 44 No.7, pp. 2047-2054, Jul. 2009